Effects of quenching media on the mechanical properties of Al-Al_2O_3 metal matrix composite

A thesis submitted in partial fulfillment of the

requirements for the degree of

Master of technology
in
Metallurgical and Materials Engineering

By

Suvin Sukumaran
(212MM1335)

Department of Metallurgical and Materials Engineering
National Institute of Technology
Rourkela
2014

Effects of quenching media on the mechanical properties of Al-Al_2O_3 metal matrix composite

A thesis submitted in partial fulfillment of the

requirements for the degree of

Master of technology
in
Metallurgical and Materials Engineering

By

Suvin Sukumaran
(212MM1335)

Under the guidance of

Prof. Bankim Chandra Ray

Department of Metallurgical and Materials Engineering
National Institute of Technology
Rourkela
2014

National Institute of Technology
Rourkela

CERTIFICATE

This is to certify that the thesis entitled, ***"Effects of quenching media on the mechanical properties of Al-Al_2O_3 metal matrix composite"*** submitted by **Suvin Sukumaran (212MM1335)** in partial fulfillment of the requirements for the award of Master of Technology Degree in Metallurgical & Materials Engineering at the National Institute of Technology, Rourkela is an authentic work carried out by him under my supervision and guidance.

To the best of my knowledge, the matter embodied in the thesis is based on candidate's own work, has not been submitted to any other University/Institute for the award of any Degree or Diploma.

Date:

Prof. Bankim Chandra Ray
Head of Department
Dept. of Metallurgical and Materials Engg.
National Institute of Technology
Rourkela – 769008

ACKNOWLEDGEMENT

I express my sincere gratitude to my guide **Prof. B. C. Ray**, Head of Department, Metallurgical and Materials Engineering Department , NIT Rourkela for his in depth supervision and guidance, constant encouragement and co-operative attitude for bringing out this thesis work. I am greatly indebted to my dear teacher **Mrs Khushbu Dash Mishra** without whom which it would have been impossible for me to complete my project work. Her constant encouragement, generosity, everlasting patience and sharing of knowledge helped me a lot to complete my research.

I would also like to acknowledge and express my gratitude towards S. Pradhan, R. Pattnaik, U. K. Sahu (laboratory members of Department), Dinesh Rathore, B. Mohan Kumar (Ph D scholars) and Kishore Kumar Mahato (Mtech Scholar) for the help I received from them.

Finally I would like to thank my parents and sister who have always been supporting me in pursuing my dreams.

Suvin Sukumaran

ABSTRACT

Considerable interest has been generated in the study of Aluminium matrix composites (AMCs) reinforced with hard ceramic particles where it is possible to obtain high specific strength and stiffness, resistance to wear and functionality at elevated temperatures. The applications of AMCs includes gears and braking system in automobiles, fuel access door covers and ventral fins in automobiles, golf club shafts, bicycle frames, track shoes in military tanks, flywheels, ice hockey sticks, cryostats, rocket turbine housing, missile nose tips etc. In the present investigation, $Al–Al_2O_3$ nano- and microcomposites with different volume fractions of alumina was fabricated using powder metallurgy route and then characterized using X-ray diffraction and scanning electron microscope succeeded by density and Vickers microhardness measurements. The heat treatment of the samples was done by first heating the composite specimens to conditioning temperatures of 150°, 200°, 250° and 300°C separately in furnace, then holding the samples at that temperature for 1 hour and finally quenching them in different media such as air, brine solution (7 wt. %), engine oil, liquid nitrogen and polymer (poly ethylene glycol-5 wt. %) solution. After quenching the microhardness values were again measured. 3-point flexural test was conducted on the quenched samples at a loading rate of 0.5 mm/min. Some of the selected fractured samples were then taken for fractography analysis using field emission scanning electron microscope (FESEM). The results revealed that the strength and hardness of the composites were significantly enhanced as a result of quenching heat treatment. Higher strength and hardness was observed for brine quenching followed by liquid nitrogen, oil, polymer and finally air cooling. The betterment of mechanical properties of AMCs after quenching can be accredited to the intensified dislocation density produced due to coefficient of thermal expansion mismatch between the particles and the matrix and also due to the back stress developed due to particles blocking the plastic flow of the Al matrix phase. The significance of study of quenching of AMCs is realized in applications such as cooling of cylinder liners and pistons in automobiles and aerospace structures which are suddenly subjected to very low temperatures at high altitudes due to presence of strong winds.

Keywords: Metal matrix composite, Quenching, Thermal misfit dislocation, Micro composite, Nano composite

Content

List of Figures

List of Tables

Chapter 1

Introduction

1.1 Background and motivation

The progress of composite materials has become a turning point in the history of science and technology as it permits the synergising of definite properties of its ingredients namely the reinforcement phase and the bulk matrix phase and suppresses the deficiencies of each of them [1]. The composite materials based on metals and their alloys which are termed as metal matrix composites (MMCs) have geared up extensive research all over the world during the past 20 years as they are found to be suitable candidate materials for structural applications in aerospace and automotive industries, defence sector and general engineering applications. The outstanding ability of MMCs to unify the reinforcement (usually ceramic material) properties (high strength and elastic modulus) with that of the metallic phase (high ductility and toughness) makes them capable of bearing higher compression and shear loadings and also sustainability at elevated temperatures [2,3].

The usage of aluminium based MMCs (AMCs) are increasing in a wide variety of industries as they provide unique advantages over conventional monolithic materials in terms of more specific strength and stiffness, improved wear resistance and high temperature capabilities, adjustable coefficient of thermal expansion (CTE) and resistance to thermal fatigue. The applications of AMCs includes gears and braking system in automobiles, fuel access door covers and ventral fins in automobiles, golf club shafts, bicycle frames, track shoes in military tanks, flywheels, ice hockey sticks, cryostats, rocket turbine housing, missile nose tips etc [4-6]. AMCs with reinforcement in the form of particles are gaining importance due to their isotropic properties when compared with fiber and whisker reinforcements which exhibit anisotropic mechanical properties. These particulate reinforced metal matrix composites (PRMMCs) exhibit high strength, hardness, wear and erosion resistance [4,7]. They have superior plastic forming potential than fiber and whisker strengthened composites which inturn reduces their manufacturing cost. The properties of PRMMCs depend upon the size and properties of the reinforcing particle, interparticle spacing, particle-matrix interface condition and shape and volume fraction of the particle [1].

PRMMCs can be fabricated through a variety of manufacturing routes such as powder metallurgy, diffusion bonding (solid state processing), stir casting, melt infiltration, spray deposition (liquid state processing) and in-situ processing techniques [8]. Powder metallurgy route is the most preferred route of fabrication for PRMMCs since it holds the advantage of

minimising the deleterious reaction between the metal and the ceramic reinforcement phase during processing. Moreover, the effect of segregation and tendency for formation of intermetallic phases are reduced in powder metallurgy processing when compared to processing in liquid state [1,9].

Heat treatment can be implemented to greatly enhance the mechanical attributes of materials. It is a critical function in the final production of most engineering components. The main purpose behind heat treatment procedure is to make the metal both structurally and physically suitable for a clearly defined application [10]. Desired values of hardness and strength in many metal alloys usually ferrous alloys are developed through proper heat treatment methods [11]. Heat treatment has also a significant impact on the hardness, strength and the wear behaviour of AMCs [12]. Most of heat treatments involve quenching stage which greatly influences the final properties of engineering components which includes specific hardness, less residual stresses and distortion, reduced likelihood of cracking etc [13]. Quenching and quenching followed by ageing heat treatment methods have proved to be beneficial for both particulate and whisker reinforced AMCs [14]. The effect of quenching is largely dependent on the quenching media or quenchant used. Producing the desired metallurgical transformation is the primary function of any quenchants. The choice of the quenching medium is governed by the size, shape and hardenability of the component. Prevention of cracking and reducing the distortion in specimen arising due to non-uniform heat transfer over the surface are also the functions of quenchants [15].

The most commonly used quenching media are water, brine and conventional oils. Water quenching has high coolong rate and produces good hardenability. But the disadvantage of water quenching is that it can generate higher residual stresses in the material which inturn will lead to distortion and cracking. Also, the prolonged duration of vapour blanket stage during quenching is also a major issue concerned with water quenchant. This can be overcomed by using aqueous solution of salts as quenchants such as brine solution which can decrease the viscosity of water and thereby reducing the duration of vapour blanket stage. Brine solution offers higher cooling rate with lesser distortion than water quenchants. But the corrosive nature of brine solution is a major limitation for their application [16]. Oil is suitable quenching medium for crack sensitive parts. It produces less distortion compared to other quenching medium such as water and brine solution. Aqueous solution of polymers such as PAG (Poly Alkylene glycol), PEG (Poly Ethylene glycol) etc. are commonly considered alternatives for oil quenchants. One of the major highlight of polymer quenchants

is their inverse solubility in which a thin film of glycol is formed around the work piece which wets it and thus suppresses the formation of vapour blanket around it and hence reduces the chances of distortion. They provide more uniform heat removal during the quenching process which inturn results in lower thermal gradients and less distortion in the components [16, 17].

PRAMCs (Particulate reinforced aluminium matrix composites) having high hardness, wear resistance and appreciable strength are required in the applications such as automobile gear parts and braking systems, fan exit guide vanes in gas turbine engine, ventral fins in military aircraft etc. Since quenching is a suitable heat treatment process for AMCs to achieve these properties, it is necessary to understand the effect of quenching and different quenching media on the strength, hardness and fracture behaviour of AMCs. Also, it is essential to know the influence of variables such as size of the particle (micro and nano), particle volume fraction and conditioning temperature on the mechanical behaviour of PRAMCs during quenching in different medium. In the present investigation the effect of quenching on the mechanical properties of Al-Al_2O_3 nano-composite and micro-composite are studied extensively.

1.2 Objectives of the research

The main objectives behind the research are:-

- To understand the effect of quenching on the strength, hardness and fracture characteristics of Al_2O_{3P}/Al nano- and micro-composite.
- To compare the strength and hardness of Al_2O_{3P}/Al nano- and micro-composite in different quenching medium such as air, brine water, oil, liquid nitrogen and polymer.
- To study the influence of change in quenching temperature on the strength and hardness of Al_2O_{3P}/Al nano- and micro-composite.
- To study the fractography of the Al_2O_{3P}/Al nano- and micro-composite samples subjected to quenching in different medium.

Chapter 2

Literature Review

2.1 Metal Matrix Composites

Considerable attention has been generated in the past decades towards research in metal matrix composites (MMC) since they present a unique distribution of mechanical and physical properties which finds numerous applications in automotive, defence and aerospace sectors. MMCs constitute a bulk matrix phase which is a metal that is bonded along the interface to usually one or more reinforcement phases which are present in lesser volume fractions. Holding the reinforcement phases intact and enabling efficient external load transfer to it are the main functions of the matrix phase. When ceramic reinforcements are incorporated in metal matrix, remarkable enhancements in strength, modulus of elasticity, wear resistance, high temperature sustainability and structural efficiency are obtained. Another advantage lies in the ability to control the physical properties including density, thermal conductivity and thermal expansion coefficients so as to adjust the properties of the material to satisfy the need the needs of its applications. Proper selection of reinforcement and matrix phase, processing techniques and heat treatment procedures are required for the suitability of MMCs for the specific applications. Aluminium based metal matrix composites (AMCs) have distinct advantages over the conventional alloys of Al which includes greater specific strength and stiffness, enhanced properties at high temperatures, controllable thermal expansion property, improved abrasion and wear resistance and damping capabilities which makes them a special class of advanced engineering materials [1,18,19].

Based on the reinforcement type used, metal matrix composites can be classified as follows:-

(1) Fiber reinforced metal matix composites

(2) Particulate reinforced metal matrix composites

(3) Whisker reinforced metal matrix composites

Fiber reinforced MMCs have reinforcements in form of fibers which have usually diameter less than 20μm. Whisker reinforced MMCs have better mechanical properties than particulate and fiber reinforced MMCs and it accomodates reinforcements with aspect ratio higher than 5, but not present in continuous form. Commercial application of whisker reinforced MMCs are limited due to health hazards imposed by them. Particulate reinforced MMCs having equi-axed reinforcement in the form of particles possess better plastic forming capability and lower manufacturing cost than whisker and fiber reinforced MMCs. Superior properties at high temperatures and improved resistance to wear are additional benefits offered by

particulate reinforced MMCs. Also they have flexibility in route of manufacturing and easy availability. The shape, size and volume percentage of the particles and their properties, interparticle spacing and conditions at the interface of particle-matrix determines the overall properties of particulate reinforced MMCs [8]. Better yield strength, modulus of elasticity and ultimate tensile strengths are observed for Al alloy matrix composites which are reinforced with particulates. Also the properties are moreover isotropic than fiber or whisker infiltrated composites. This makes them appropriate for use in structural components. The resistance to wear and abrasion are extremely good for particulate reinforced MMCs. The effectiveness of load transfer which affects the strengthening of the composite is governed by the matrix-particle interface strength. It is also an important factor which determines the ease of decohesion, which will affect the failure mechanism of the composite [20].

Particle size and volume percentage are the two important parameters which are related to the particulate reinforcement. Generally by increasing the volume percentage of particles there would be increment in the strength since larger number of dislocation barriers are created, but ductility will get reduced. The reduction in ductility occurs due to the localisation of deformation on a smaller volume of the matrix. Reducing particle size can also increase strength since larger numbers of particles are present for the same volume fraction. The ductility remains unaffected because once the size goes below a critical value; there won't be further fracture of the particles. Adding to this there would be also further improvement in strength from mechanisms such as Orowan strengthening and pinning of the grain boundaries by the particles [21,22].

Common reinforcements which are used for AMCs include alumina, silicon carbide, titanium carbide, boron carbide and graphite. Among these alumina has high specific stiffness, better high temperature properties and excellent oxidation resistance. It is also available at low cost. Generally for applications demanding good wear resistance and strength, alumina of about 30 volume percentages are used. However, volume percentage greater than 70% is used for electronic applications. Finer particles with lower interparticle spacing are generally preferred for obtaining optimum strength. When load is applied at room temperature, dislocations will be generated and they get pushed through the spaces between the particles. With the advancement in nanotechnology, nanometric particulates exhibiting attractive properties are now readily available [14,23-25].

2.2 Fabrication by powder metallurgy

Fabrication of MMCs can be made possible either in the solid state or in liquid state. Powder metallurgy is a common route of fabrication that is employed for particulate reinforced aluminium matrix composites. However, various methods such as in-situ processing, infiltration technique and stir casting are available for particulate composite fabrication in the liquid state. The percentage of reinforcement added and its nature mainly dictates the suitable fabrication procedure that can be adopted for it [26]. Better mechanical properties can be obtained for particle strengthened composites when solid state fabrication techniques are used for their production. Solid state processing can nullify the harmful side effects of melting techniques of fabrication which includes chances of segregation and occurrence of intermetallic phases. The probability of reactions occurring between the ceramic particle phase and the metal can be avoided to a larger extent if the solid state fabrication route is employed [27].

2.3 Strengthening mechanisms in PRMMCs

Even with using particles which have superior properties, it is not possible to effectiviely transfer the load from the matrix to it through the interface. So, for explaining the strengthening of MMCs due to particle inclusion, a simple concept based on stress transfer mechanisms cannot be solely employed.

1. Strain hardening

The dramatic increase in the number of dislocation-dislocation interactions facilitates strain hardening which reduces dislocation mobility. So, larger stresses are required for further deformation to take place. Thus it increases the strength and hardness of the composites. The variation of strength of metal crystals as a function of dislocation density is shown in the figure below.

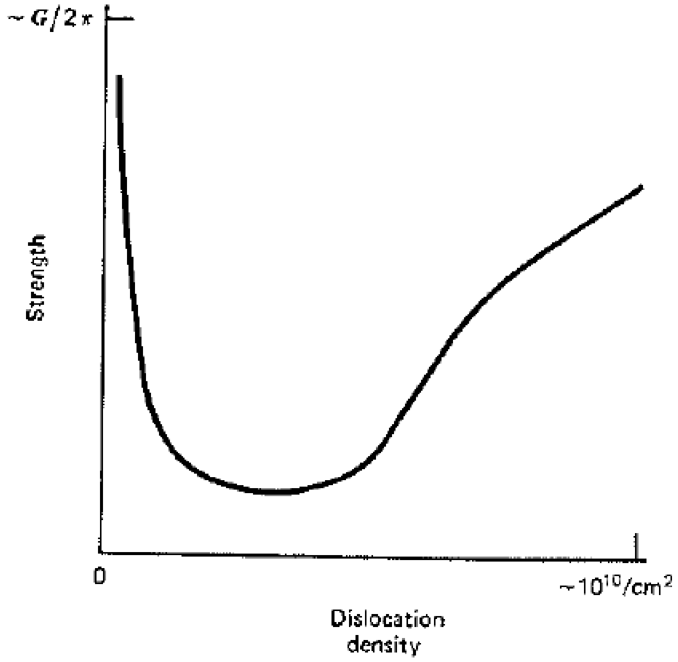

Fig. 2.1 Strength of metal crystals as a function of dislocation density.

2. Grain boundary strengthening

This strengthening occurs when the grain boundary operates as a barrier to the motion of glide dislocations. In PRMMCs, the particles inhibit the grain growth of the matrix by pinning down of dislocations at the grain boundaries. So grain refinement occurs which enhances both the strength and toughness of the composite. The relation between the grain size and yield stress of polycrystalline material is given by the Hall-petch relation which is given by,

$$\sigma_{ys} = \sigma_i + K_y d^{-0.5} \quad \ldots\ldots (1)$$

Where, σ_i – overall resistance offered by the lattice to the movement of dislocations

K_y – Locking parameter which measure the respective hardening contribution of grain boundary

d – grain diameter

3. Solid solution strengthening

The restriction of dislocation movement due to the presence of solute atoms constitutes solid solution strengthening which usually occurs in matrix alloys. Interaction occurs between the strain fields of the solute atoms and the dislocations present in the lattice.

4. Precipitation hardening

Precipitates nucleate in the matrix alloy when the solute concentration exceeds the solubility limit. These precipitates obstruct the dislocation motion and thus strengthen the composite. The nucleation and growth of these precipitates depend on the solutionizing temperature, cooling rate and the ageing kinetics.

5. Dispersion strengthening

The particles acts as barrier to the dislocation motion and facilitates looping of the dislocation around them. This is known as orowan bowing mechanism. Once a dislocation passes through the particles, residual loops of dislocations are formed around each particle.

Orowan strengthening is given by Gb/l, where G is the modulus of rigidity of the matrix, b is the Burgers vector, and l the particle spacing [28]

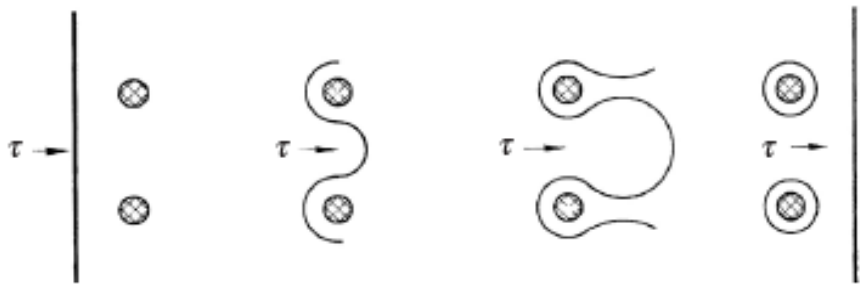

Fig. 2.2 Dislocation looping around particles

2.4 Type of stresses in MMC

The various types of stresses that can be produced in a MMC are: (i) the stresses which are generated due to the difference in the elastic properties of the matrix phase and the reinforcement phase. It is being accommodated as a load transfer term. These types of stresses elevate the reinforcement load factor and deteriorate the matrix stress. The second type of stress present in the MMC is (ii) macroscopic stress which can be generated either thermally or applied mechanically. The third type of stresses arises due to the misfit strains between the two constituent phases. These misfits can be produced during cases such as cooling from higher temperatures where the strain is generated to compensate for the difference in thermal expansivities of the ceramic and metal phase.

The stresses which are present in a material even in the absence of external force can be termed as residual stresses. These stresses can vary on a long range which can encompass distances which are even greater than the grain size of the material. Also, short range order residual stresses are also present which are usually associated with dislocations and vacancies. Also the presence of precipitates at a finer scale can effectively contribute to these kinds of micro residual stresses that can significantly alter the attributes of the matrix material. Residual thermal stresses are often developed as a result of quenching heat treatment due to large difference in temperature existing between the conditioning temperature and the bath temperature. If the amount of these residual stresses is more, they can adversely affect the failure behaviour of the material by causing distortion and cracking [29]. Thermal stresses are generated at temperatures other than that associated with fabrication process; such stresses will vary directly with differences in thermal expansivities existing between the matrix and the reinforcement. The expression for these thermal stresses is given by:

$\sigma = E\Delta\alpha\Delta T\ /(1-\mu)$ …… (2)

Where, $\Delta\alpha = \alpha_m - \alpha_r$

E- modulus of elasticity

μ- poissons ratio

α_m –matrix thermal expansion coefficient

α_r –reinforcement thermal expansion coefficient

ΔT – change in temperature

2.5 Failure mechanisms in PRMMCs

The fracture response of PRMMCs depends mainly on the respective strengths of the matrix phase and the particl phase. The state of heat treatment also exerts influence on the failure mechanism of PRMMC. The particles which have sizes greater than 1500nm are generally subjected to cracking when the stress is concentrated upon them. However, smaller size particles with particle size less than 200nm does not crack and bonds well with the matrix phases. The medium size particles having sizes in the range 200-1500nm are more susceptible to interface decohesion [23,24].

The main failure mechanisms operating in PRMMCs are interfacial de-cohesion, particle cracking and marix cracking. The ductile mode of failure is described by microvoid coalescence where the microvoids nucleate, grow and finally coalesce into large cracks. Most of the fracture energy associated with microvoid coalescence is consumed during the growth

of the microvoids. Ductile fractures exhibit unique structures referred to as ductile dimples. They are usually hemispheroidal in shape. They generally form cup shaped equiaxed dimples when the plastic strain is uniform in the direction of the applied load. Brittle fracture modes are generally subclassified into two types namely intergranular fracture and transgranular fracture. The crack propagates between the grains of the metal in intergranular fracture. It produces a rock-candy or faceted appearance. Trandgranular fracture propagates through the metal grains and present a flat, bright appearance. Cleavage and fatigue mode of failure comes under transgranular fracture.

Griffith crack theory

Griffith crack theory states the condition for crack propagation in brittle materials. The crack growth will be unstable when the elastic strain energy which is released through crack growth is enough to provide the energy needed to produce new crack surface. Griffith criterion cannot be applied for highly ductile materials since before the stress intensity present at the crack tip can be effectively decreased through plastic deformation. This theory provides proper justification for the observed low fracture strength in materials when compared to their theoretical cohesive strength. The presence of large number of flaws in the material reduces their strength to failure. Weibull modulus gives an approximate value for the scatter in the fracture strength due to the presence of these flaws. The mathematical formulation for Griffith's theory is given by,

$$\sigma = \sqrt{2E\gamma_s}/\pi a \quad \text{…………………………………………………………….. (3)}$$

Where, σ -applied stress

a- one half crack length

t- thickness

E- Youngs modulus

γ_s – Specific surface energy

Fracture strength of MMCs can be increased due to the blunting of the crack tip by the presence of the particles [28].

2.6 Quenching heat treatment

Heat treatment procedures can substantially vary the properties of metals, alloys and composites. The cooling stage starting from the conditioning temperature to ambient

temperature can significantly alter the mechanical properties of the material. Internal stress level is affected by the cooling rate. It also dictates the non-equilibrium state which is exhibited by the metallographic structures. The three steps generally involved in the heat treatment of aluminium alloys are solutionizing heat treatment, quenching and artificial aging. The most important stage is quenching. The generation of the desired microstructure and required physical properties can be achieved with the help of quenching which is basically a controlled cooling procedure from a higher temperature to a lower temperature. A typing example for quenching is in the case of martensite formation in steel. The steel is first heated to the asutenizing temperature. Then after holding it at that temperature for some time, it is quenched in cold water rapidly so as to minimize the formation of undesirable microstructures such as pearlite, and maximize the formation of hard and brittle martensite microstructure. Residual stress generation, cracking and distortion effects must be minimized during quenching to a larger extent so as to produce more improved mechanical properties in the material.

In many metal alloys mainly ferrous alloys and carbon steels, quenching heat treatment is done to achieve the desired microstructure, hardness and strength. After quenching to maximum possible hardness, another heat treatment process called tempering is employed to bring the ductility factor also to the material so as to make it suitable for practical industrial applications. So a unique combination of hardness and ductility is achieved with the implementation of quenching and tempering heat treatment cycle. Improving the uniformity of cooling process throughout the quenching process is also an important function of the quenchant in addition to obtaining the required microstructural modification. The control of the severe distortion and cracking tendency in the workpiece during quenching can be achieved only by studying how the parameters associated with the quenching directs the outcome of the post quenching properties [16].

2.6.1 Strengthening due to quenching

One interesting observation regarding the particulate reinforced composite materials is that heat treatment effect has a substantially larger impact on the deformation behaviour of composites than other parameters such as particulate geometry and volume percentage [30]. The strengthening of particulate reinforced metal matrix composites by quenching can be ascribed to mainly two mechanisms which are:- (i) Punched-out dislocations developed as a result of CTE mismatch between the matrix and the reinforcement, (ii) Back stress developed by virtue of particle obstructing the plastic flow of the matrix. It has been reported that the major parameters that are influencing the increase in flow stress during quenching heat

treatment are the thermal gradient, conditioning temperature, particulate size and volume fraction [30]. With the increment in quenching temperature, there would be also an enhancement in the strengthening of MMC due to CTE mismatch. Strengthening due to back stress was influenced by yield strength of the matrix in addition to the final temperature of quenching [31]. In MMCs, due to large difference in the thermal expansivities between the matrix material and reinforcement, internal residual stresses would be generated which are larger enough to produce dislocations at the interfacial region. These dislocations could possibly emerge from anywhere around the particle once sufficient cooling has taken place. Along with the effect of quenched-in vacancies and increased dislocation density, the effect of dissolution of the reaction products also influences the mechanical properties after quenching in the case of metal alloy reinforced composites.

2.6.2 Quenchants

Water, brine solution and polymers are the quenching media which are generally implemented for aluminium alloys [18]. Water and oil are the simplest and widely used quenching media. Prominent enhancement in the cooling properties of these two media can be modified by incorporating salts, acids, alkalis and other chemical compound addition to water. Aqueous solutions incorporating emulsions water and oil are also used. In the literature, to achieve cooling rates in between that of oil and water, concentrated sulphuric acid has also been considered. But it has severe limitations due to its hydroscopic nature. So maintaining its concentration level is extremely difficult. Also further danger to workers from its splashing is also a concern. To achieve intermediate cooling rates between oil and water other alternatives considered are hot aqueous solutions and hot water bath. Proper agitation and circulation is required for the stability of these quenchants. The concentration and the temperature must also be accurately controlled for their effectiveness. Another quenching media used in research are glycerine solutions which is a suitable alternative for commonly used water and oil. Also it was reported that using sodium silicate solutions as quenching medium can provide desired attributes intermediate to that of oil and water. They are cheap and resists corrosion tendency of steel. But their utility as a quenching medium is limited by their tendency for formation of thin silica layer coating of silica on quenched workpiece surface. Also these sodium silicate solutions are highly unstable. Polymer solutions having higher molecular weight are generally being used for quenching heat treatment of metal alloys. The miscibility of polymer with water offers advantages including protection from oil-fire hazard danger. But one of the major limitation of polymer quenchants is that their

increased concentration can often lead to overall decrement in the cooling power since the vapour blanket is formed for an extended duration during the course of quenching [32]. Polymer quenchants have also emerged as a suitable alternative to obtain cooling rates intermediate to that of oil and water. Also, the generation of thermal residual stresses are minimized when the polymer quenchants are used [33]. Polyalkylene glycol quenchants were used in the mid 1960s for the aluminium heat treatment industry which effectively reduced the distortions in them during quenching [34]. Also it was reported that in the case of polymer quenching, the vapour blanket stage can be re-established with the increase in concentration of the polymer which can adversely affect the cooling potential of the quenchant. Lower amount of polymer quenchant can effectively reduce the maximum surface heat transfer coefficient and hence lead to the blocking of vapour blanket stage during the early stage of quenching. When the concentration of polymer quenchant was increased from 5% to 20%, no effect was observed on the maximum surface heat transfer coefficient [35]. The cooling power of aqueous polymer solutions is observed to increases with the level of agitation, but would tend to decrease with increasing quenching temperatures and concentration of the polymer which would profoundly influence the stages of quenching. Eventhough the wettability of aqueous media is poor due to their low contact angles; their quench severity is higher than that of oil media. Decrement in the Rockwell hardness value was observed during quenching of carbon steel in poly ethylene glycol as the concentration of PEG was increased from 20 vol. % to 100 vol. %. Decreasing the PEG concentration depicted improvement in the hardness and also the variation in hardness from the centre to the surface of the workpiece was also substantially decreased. It was also noticed that the effect of increasing the temperature has added only a mild improvement in the cooling rate. The influence of temperature on cooling rate was less visible at high concentrations of the polymer. Non uniform cooling tendency was seen from the surface to centre of the specimen. The centre cools at a slower rate than the surface [36].

Unacceptable degree of distortion is seen during cold water quenching which is attributed to their high thermal gradients. One remedy is to use hot water in the temperature of about 60-70 °C as the medium for quenching. This will effectively reduce the thermal gradient. Also the problem associated with the cracking of the workpiece is also eliminated to a certain extent. But the rate of cooling will be less here which will affect the mechanical properties. High cooling rates can be achieved through quenching work pieces into liquid nitrogen. Liquid nitrogen has also been used as a quenching medium as it is a safe, cheap and harmless

cryogenic fluid which can achieve very high cooling rate. Liquid nitrogen quenching study is useful in the areas of food engineering and cryobiology. The maximum cooling rate obtained using liquid nitrogen can go it the range of 2000 to 8200 Ks^{-1} [37]. It has been reported that cooling rate during quenching in liquid nitrogen was found to be only 1.8-2.3 times than that of quenching in static air [38]. Judicious and careful selection of the quenching medium is critical for attaining optimum mechanical attributes in the material and to avoid the generation of quench cracks and distortion in the workpiece. For reducing the residual stresses in components having large variation in section thickness, the cooling rate must be kept low. For this purpose oil quenchants whose quench severity is less are found to be appropriate. But since they are non-renewable sources, they can bring about to air and water pollution [39].

2.6.3 Stages in quenching

There are basically three types of cooling mechanisms present during quenching of workpieces which includes film boiling (slower cooling rate), nucleate boiling (faster cooling rate) and convective cooling (slower cooling rate). Thermal gradients will definitely be induced due to the different cooling rates exhibited by these three mechanisms. These can further lead to increased generation of residual thermal stresses and transformational stresses which if present in a larger amount can lead to severe distortion and cracking in the workpiece.

The three stages during the quenching process are shown in the figure below on a typical cooling curve. Vapour blanket stage or film boiling is the primary stage which is followed by nucleate boiling stage and finally convective stage. Also the curve for cooling rate associated with the quench is also shown for comparison. The vapour blanket stage (1 in figure) is initiated on the contact of the workpiece with quenching medium whereby a blanket of vapour covers the workpiece. The blanket formation occurs when the heat supply from the surface of the workpiece exceeds the heat needed for the formation of maximum vapour per unit area on the workpiece. The rate of cooling will be slow during this stage due to the thermal insulation property of the vapour around the workpiece. The combined mode of conduction and radiation heat transfer occurs during this stage along the vapour. After sometime as the workpiece cools down, breaking down of the vapour blanket stage takes place and the temperature T_{vb} at which this occurs is termed as Leidenfrost point. At the course of this transition regime, some parts of workpiece will experience film boiling whereas in other regions there would be the onset of nucleate boiling. The nucleate boiling

stage shown as 2 in figure is characterised by violent boiling of the quenching medium due to the enhanced formation of bubbles in the surface of the specimen. Direct contact is established between the fluid and the workpiece during nucleate boiling stage. Rapid transfer of heat takes place during this stage. The temperature differential existing between the quenching media and the workpiece provides the driving force for nucleating bubbles on the specimen surface. With further cooling of the workpiece there will be decrement in this driving force which results in lesser number of bubble formations. So there would be further reduction in the heat transfer coefficients with lowering temperature. The convective stage (shown as 3 in figure) starts when the temperature of the workpiece falls below the boiling point of the quenchant. At this temperature the nucleate boiling stage cannot continue as a result of low surface temperature. The heat transfer rate remains to be slow during convective stage also similar to the vapour blanket stage. In this stage the process of dissipation of heat takes place from the workpiece by the bulk movement of the quenching medium. Crucial role is played by the difference between the actual temperature and boiling point of the medium in determining the heat dissipation rate in case of liquid quenching mediums. Another major important factor influencing the cooling potential of liquid quenchants is their coefficient of viscosity. Generally if the viscosity is less, then the rate of heat dissipation will be faster. The cooling rate is given by the slope of the cooling curve. From the figure it can be easily deducted that film boiling and convection stage have lower rate of cooling as their slope is less compared to nucleate boiling stage [16,40].

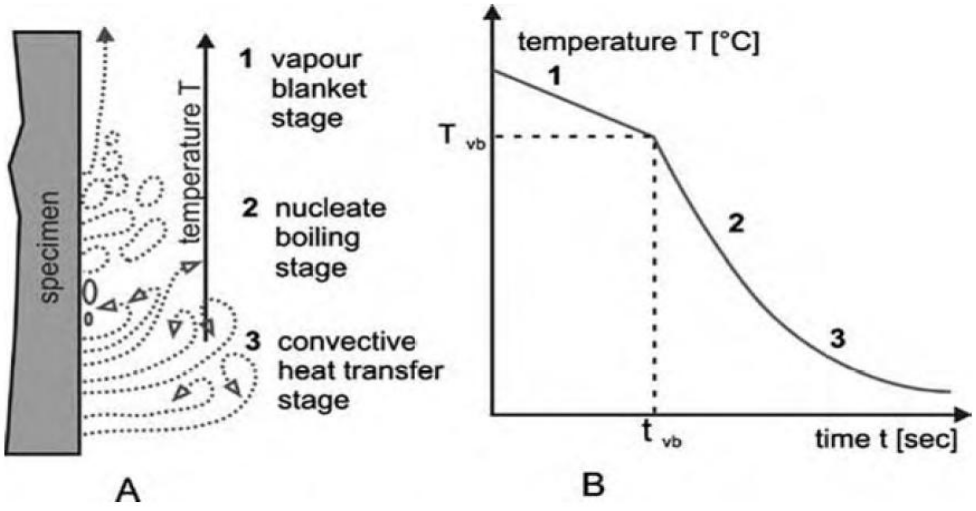

Fig. 2.3 (A) Illustration of the three stages of quenching present near the specimen, (B)Typical cooling curve showing the stages of quenching

One of the major factors promoting the induction of residual stress is the non-uniform cooling and phase transformation that is taking place during the quenching process. The progression of heat transfer is possible only through the surface of the quenched specimen [41,42]. Also phase transformation has a higher chance to occur while slow cooling. By maintaining a degree of control over the quenching parameters such as the holding temperature, time and agitation level, it is possible to accurately assess the thermal history of cooling during rapid quenching. Elevation in the bath temperature can cause decrement in cooling efficiency due to the prolonged period of vapour blanket stage in quenching. When temperature approaches the boiling point, water will vapourise and the resultant vapour forms a blanket over the workpiece severely reducing its cooling rate. The level of agitation enhancement can significantly elevate the heat transfer rate during the quenching process independent of the bath temperature. Breaking down of the vapour blanket stage and introduction to nucleate boiling is easier if properly agitated. More rapid cooling rate is introduced into the system as a result of agitation. Also formation of bubbles during agitation while the boiling stage can further improve the heat transfer rate from the workpiece. Uniform circulation of cool water along the surface of the wokpiece is achieved due to agitation which always maintains a higher temperature gradient between the quenching medium and the surface. This results in greater degree of heat dissipation. It is difficult to control and optimize heat treatment procedures such as quenching or surface hardening (rapid heating). Restriction of phase transformations are critical for achieving desired thermal gradients and mechanical properties in the work piece [43].

2.6.4 Quenching of MMCs

Noteworthy enhancement in the ultimate tensile strength of Al-SiC_p was observed due to quenching treatment in water. The dislocations were observed to punch out into the matrix from the interface, when Al-SiC_p composites were quenched in water. The punching distance was directly proportional to the temperature drop during heat treatment [44]. Sharma et al. [18] studied the age hardening behaviour of Al-4.5wt. %Cu/zircon sand composite quenched in different media such as water, oil and 7 wt. % salt brine solution. Higher cooling rate and strength was observed in salt brine quenching followed by water and oil quenching. Specimens quenched in water took duration time to achieve peak hardness inspite of having higher dislocation forming tendency. This was attributed to the greater chance of dislocation annihilation taking place. The probability of dislocation annihilation and interaction is increased by higher dislocation forming tendency of water quenched samples. Cracking and distortion was observed to be higher for salt brine quenched samples. High dislocation

density was observed in water quenching of SiC_p reinforced 2124 aluminium matrix composite which were generated due to the CTE difference between the particle and the matrix [45]. Enhancement of strength and hardness was observed due to water quenching in in-situ TiB_w reinforced Ti6Al4V alloy matrix composite with network architecture [46].
It has also been pointed out in the literature that in addition to the strengthening of MMC resulting from the CTE mismatch and back stress generated, there is also possible strengthening effect realised from the quenched in defects, especially vacancies due to rapid quenching from high temperature. These defects will gradually become obsolete with further annealing heat treatment [43]. If the concentration of point defects generated due to rapid quenching from elevated temperatures is higher, then low temperature clustering will be effective [47]. These point defects can also lead to the decrement in electrical resistivity of pure aluminium after the quenching [48]. When pure aluminium was heated to a temperature of 600°C and quenched in cold ice water after maintaining a holding time of 10 minutes, enhancement in the hardness was observed. This was attributed to the development of dislocation loops which are generated due to the quenched-in vacancies or vacancy clusters resulted from rapid quenching process. Also formation of jogs was observed which could also lead to the hardening effect by elevating the yield stress. The superior stacking fault energy of aluminium also promotes the jog formation during quenching. Higher work hardening rate was observed for the air cooled specimens. This is because of the localisation of plastic deformation resulting from dislocation channelling in quenched metals [49].

The large number of dislocations generated due to quenching can substantially enhance the pile-up stresses which are resulted from the geometrically required dislocations during plastic flow. This can possibly lead to fracture of the particles [31]. Higher dislocation density was observed near the interface region of SiC particulate reinforced Al matrix composite when they were quenched in brine solution and subsequently subjected to ageing in an oil bath at 180°C followed by room temperature ageing [50]. Studies using a viscoelastic-plastic mathematical model were conducted to predict the residual strain development in a steel plate subjected to quenching in a 25% Aqua quench polymer solution from a holding temperature of 850°C. It was found that only negligibly low amount of residual strain were generated due to the quenching process even though the quenching rates were high. The effect of transformation plasticity and viscosity effects on the stress field generated can possibly account for this behaviour. Interfacial heat treansfer coefficient (h) or interfacial heat flux (q) can be used to quantify the heat dissipation from the metal during quenching [51].

Higher values of yield strength and hardness were observed in specimens quenched in water compared to oil quenched ones. But higher impact strength which is an indication of greater toughness was observed in the oil quenched specimens than the water quenched samples [52]. It was reported that quenching followed by ageing heat treatment was effective in improving simultaneously the yield strength and ultimate strength of Al_2O_3-SiO_2 short fiber reinforced Al-Si composites [53]. The density of dislocations produced due to quenching from solution treatment temperature (500 °C) to temperature of ice-cold water (0°C) can be calculated using the following equation,

$$\left(BV_p\varepsilon\right)\rho = \mathrm{bt}\,(1 - \mathrm{V_p}) \quad \ldots\ldots\ldots\ldots\ldots\ldots\ldots\ldots\ldots\ldots\ldots\ldots \quad (4)$$

Where, b is the burgers vector, B is a constant having value between 4 and 12, ε is the mismatch strain and t is the smallest dimension of the reinforcement. It has been reported that the composites will take longer duration to achieve peak hardness than the alloy which can be possibly due to a lower vacancy concentration, inadequate dislocation density in the matrix and large-scale segregation of alloying elements in the interfacial region [54]. Less fracture chances are experienced during quenching if the smaller ductile grains can effectively link with larger brittle grains in case of a dual phase structure containing both finer brittle and ductile phases [55]. Interface region hosts more quenched –in dislocations due to CTE mismatch than rest of the matrix region [56]. The pre-deformation applied to the composite before the ageing treatment can accelerate the process of age hardening phenomenon in SiC reinforced aluminium alloy matrix composites due to higher generation of dislocation density. The increase in the volume fraction of the particulates can also significantly improve the age hardening kinetics [57]. The quenching rate affects not only the strength but also the ductility. When the quenching rate is low, the vacancies will move and partly cluster with the aluminium matrix and partly disappear out of the matrix by diffusing into the surfaces [58].The time to attain peak hardness was found to be reducing with smaller SiC particle size which can be ascribed to the faster diffusion tendency of solute atoms in the matrix because of higher dislocation tendency [59].

Solute dislocation interaction developed after quenching increases yield strength and strain-hardening rate for commercially pure aluminium matrix composite. CTE mismatch strains are mostly relieved by the generation of dislocations, despite whether the specimen is furnace cooled or water quenched. The generation of thermal misfit dislocations will be more difficult

at lower temperatures due to the increased effect of back stresses and frictional stresses [23]. Quench sensitivity can be described as the change in magnitude of the as-quenched properties or precipitation behaviour with the change in cooling rate. It is exhibited by both aluminium alloys and AMCs. Due to the annihilation of vacancies at dislocations, the effect of vacancy/GPB zone will be retarded in the case of MMCs [60].

If the increase in flow stress due to quenching occurs as a result of high density of dislocations introduced due to CTE mismatch, then further external loading will decrease the dislocation generation rate. This will consequently result in a lower hardening rate. If the flow stress increment is via quenched-in vacancies, then during loading the hardening effect would be minimal as the vacancies are swept away during the initial stages of deformation. The dislocation recovery rate would be lower for cases where the solute-dislocation interactions are responsible for the enhancement in flow stress. The possible reason could be the difficulty experienced for the cross-slip of dislocations due to the friction stress of the solute atoms. Increase in hardening rate was observed with increasing quenching temperature. When quenched from very high temperatures, there would be enhancement in flow stress since the aluminium matrix would be supersaturated with impurities. The yield strength obtained was observed to be similar in the slow cooled and quenched composites which are an indication that the rate of cooling has no prominent influence on the dislocation density produced by the CTE misfit in this particular context. So sufficient caution must be exercised while interpreting the quench hardening and strengthening of commercially pure AMC since here enhancement in yield stress with quenching is primarily due to supersaturation of the matrix with impurities, not due to rise in the dislocation density. The generation of dislocations would be lower at temperatures below room temperature due to the effect of large particle back stresses and friction stresses which are present due to the dislocation density already introduced. Moreover, the strength of the matrix would also increase as temperature goes down which would make it very difficult to generate further dislocations. Random distribution of dislocations in the matrix would provide more effective relaxation of the residual stresses developed in the composites due to CTE misfit [61].

Higher quenching temperature will yield more generation of excess vacancies during quenching. Also, the segregation of supersaturated vacancies around a dislocation line can lead to the formation of jogs in a non equilibrium nucleation process [46]. The introduction of vacancies can also accelerate the grain boundary relaxation by increasing the atomic mobility in the boundaries [62]. It was reported that slowly cooled commercially pure AMCs contains

only dislocation densities marginally greater than in the monolithic matrix, which implies that there is possibility of diffusional relaxation down to temperature of around 200°C. But rapid cooling would provide relaxation of the thermal misfit strain at the interface by the generation of the dislocations and here diffusional relaxation won't take place [30]. The enhancement in the ultimate tensile strength of AMCs observed due to quenching heat treatment can be attributed to several factors including the fabrication route followed, particle geometry and distribution and also the oxygen content of the composite [44].

2.7 Some practical implications of quenching of MMCs

a. Cooling of automotive cylinder and piston: - Al based PRMMCs find applications in automotive pistons and cylinders. Very high temperature is generated inside the cylinder walls and the piston due to the exothermic combustion process that is taking place inside the cylinder. When cool water is supplied to the cylinder walls for cooling them, they are suddenly subjected to a very low temperature; i.e., a quenching process. So a crucial understanding of the quenching behaviour of the material is required.
b. Aircrafts at high altitudes facing strong winds: - The aircraft engine components made of PRMMCs which are operating at a hot temperature is suddenly subjected to a lower temperature as it elevates at a higher altitudes where strong gusts of wind are blowing. This is also an example of quenching.

c. Spacecrafts subjected to low temperature in space: - Spacecrafts whose fuselage frames and waveguides are made of MMCs are often suddenly subjected to extremely low temperatures during their journey in space which is basically a quenching process.
d. Achieving desired hardness and wear resistance in automotive gear parts and brake systems: - PRMMCs are also candidate materials for automobile gears and braking system which require superior hardness and resistance to wear which can be achieved through quenching process.

Chapter 3

Experimental details

3.1 Introduction

This chapter deals with the materials, equipments and experimental methods adopted for the research. The experimental study focuses on the effect of quenching heat treatment on the flexural strength, hardness and fracture behaviour of alumina (Al_2O_3) particulate reinforced pure aluminium (Al) matrix composites which are fabricated using conventional powder metallurgy route. Both micro-composite (micro-sized alumina reinforced AMC) and nano-composite (nano-sized alumina reinforced AMC) were considered for the study. 1, 3 and 5 vol. % of nano-alumina particles were dispersed in aluminium matrix to fabricate nano-composites whereas 5, 10 and 20 vol. % of micro-alumina particles were dispersed in aluminium matrix to make micro-composites. Phase analysis was conducted using x-ray diffractometer (XRD), and scanning electron microscope (SEM) was used to study the microstructure. Heat treatment was conducted on the samples by heating them in a furnace upto a certain temperature, holding it for 1 hour and then quenching them in air, brine water, engine oil, liquid nitrogen and polymer separately. Quenching was done in four conditioning temperatures such as 150°, 200°, 250° and 300°C. The quenched samples were then subjected to mechanical testing which includes Vickers micro-hardness test and 3-point bend test. After mechanical characterization, some selected samples were subjected to fracture analysis with the help of high resolution field emission scanning electron microscopy (FESEM). The experimental methods along with their technical specifications are discussed below.

3.2 Fabrication of samples

3.2.1 Starting materials

Pure aluminium powder (Loba Chemie, purity > 99.7%, average size~22μm) was used as the matrix. Alumina powders (Sigma Aldrich, average size~10μm (micro) and <50 nm (nano)) were used as reinforcement.

3.2.2 Blending

The compositions selected for nano-composites were 1, 3 and 5 vol. % of nano-alumina in aluminium matrix. The compositions selected for micro-composites were 5, 10 and 20 vol. % of micro-alumina in aluminium matrix. For the uniform distribution of reinforcement particles in the aluminium matrix, blending of each composition was carried out separately using a turbula shaker mixer (T2F, LCR Hi Tester, Switzerland) at speed of 45rpm for 8 hours.

3.2.3 Compaction

Compaction of the blended powders was carried out at an applied pressure of 400MPa for rectangular pellets and 200MPa for cylindrical pellets in an electrically operated uniaxial

hydraulic press (Soil Lab). Stainless steel die having an internal diameter of 10mm was used for preparing the cylindrical pellets for microstructural characterization and micro-hardness measurement. Rectangular pellets having dimensions of 31.5x12.7x6.3 mm^3 required for 3-point bend testing as per ASTM B 925-08 standard were prepared using a rectangular stainless steel die. Graphite paste was added as lubricant in rectangular die and zinc stearate powder was used as lubricant in cylindrical die to prevent the sticking of aluminium powder onto the walls of the die during compaction. Two minute holding time was provided at the applied pressure for minimizing the effect of back stress during compaction.

3.2.4 Sintering

A super kanthal heated tubular furnace (Naskar, India) was used for sintering the compacted pellets. Sintering was done in argon atmosphere to prevent oxidation during heating. The pellets were sintered to a temperature of 580°C at a heating rate of 5°C/minute and kept at that temperature for a certain period of holding time. The holding time was 60mins for cylindrical pellets and 90mins for rectangular pellets and then the pellets were allowed to cool down to the room temperature within the furnace.

3.3 Characterization of sample

3.3.1 X-Ray Diffraction (XRD)

The identification of the phases present and their crystal structure in both sintered nano- and micro-composite was done using a X-Ray diffractometer (PANalytical model: DY-1656). The scan range was 20°-80° and the step size was 2°/minute. Cu-Kα radiation having wavelength of 1.5418 A° was used for obtaining the diffraction pattern.

3.3.2 Scanning Electron Microscopy (SEM)

The micrographs of quenched cylindrical pellets were obtained using scanning electron microscope (JEOL JSM 6480 LV) which can provide magnifications upto 10,000X.

3.4 Physical property analysis

3.4.1 Density measurement

Archimedes method was used to measure the sintered density of the cylindrical pellets. Contech CB series analytical electronic balance equipped with a density measurement kit was used for this purpose.

3.5 Quenching heat treatment

Quenching heat treatment of the samples was done by first heating the cylindrical and rectangular pellets to conditioning temperatures of 150°, 200°, 250° and 300°C separately in furnace, then holding the samples at that temperature for 1 hour and finally quenching them into the following quenching medium.

- Brine water (7wt. %)
- Engine oil (Castrol)
- Liquid nitrogen
- Poly ethylene glycol (PEG) (5vol. %)

3.6 Mechanical Testing

3.6.1 Micro hardness test

Vickers hardness tester (Leco Microhardness Tester LM248AT) was used for measuring the micro-hardness of the polished cylindrical pellets of nano- and micro-composites. The load applied was 300gf and the dwell time was 5 seconds. The readings were taken four times at different locations for each specimen.

3.6.2 3-point flexural test

3-point flexural testing of the quenched rectangular pellets having dimensions of 31.5 x12.7 x 6.3 mm^3, as per ASTM standard B925-08 were carried out in universal testing machine (INSTRON-5967). The crosshead speed was kept at 0.5mm/min and the span length was maintained at 26mm.

3.7 Fractography

3.7.1 Field Emission Scanning Electron Microscope (FESEM)

The fractographs of the selected fractured 3-point bend test specimens were carried out using a high resolution field emission scanning electron microscope (NOVA NANO SEM 450) which can provide magnification upto 2, 00,000X.

Chapter 4

Results and discussion

4.1 Sample Characterization

4.1.1 X-Ray Diffraction

4.1.1.1 Nanocomposite

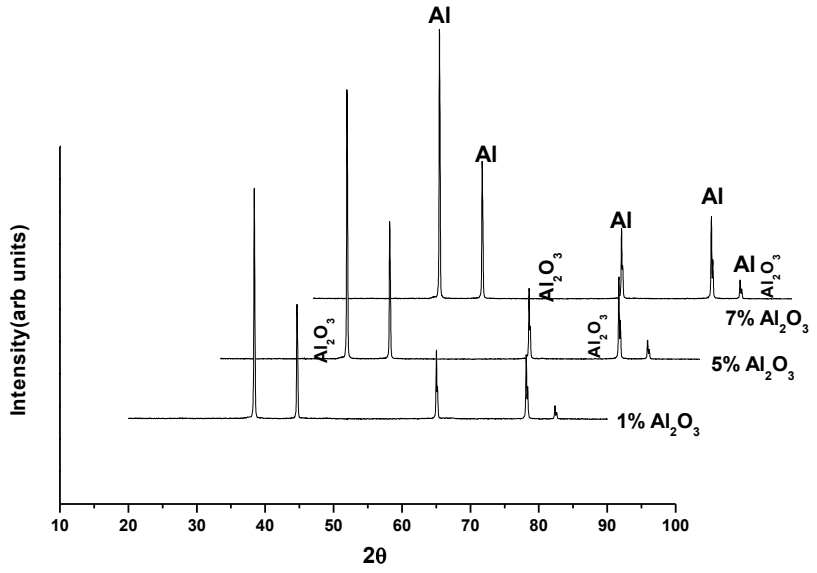

Fig. 4.1 X-ray diffraction patterns of as fabricated Al-Al_2O_3 nanocomposites

Fig. 4.1 depicts the X-ray diffraction pattern of powder metallurgy fabricated Al-Al_2O_3 nanocomposites. From that analysis of the peaks it can be observed that there are two phases present in the nanocomposite; which are the Al matrix phase and the reinforcement Al_2O_3 phase. There are no other intermediate phases produced during fabrication. Some small peaks of alumina can be clearly identified in the XRD pattern of 7 vol. % nanocomposite. At lower volume fractions such as 1 vol. % alumina, it is difficult to see the peaks produced by them.

4.1.1.2 Microcomposite

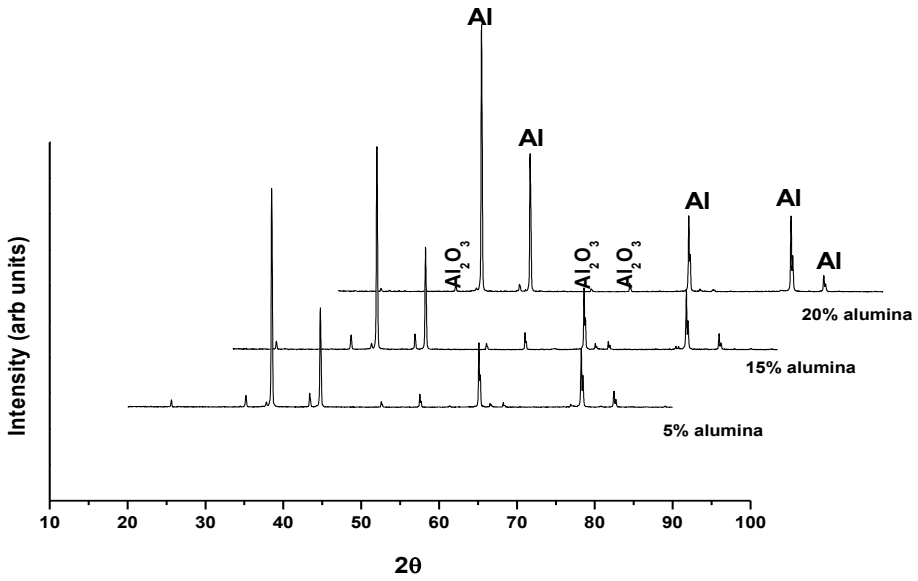

Fig. 4.2 X-ray diffraction patterns of as fabricated Al-Al_2O_3 microcomposites

Similar to nanocomposites, in the case of as-fabricated microcomposites also only the Al and alumina phases are identified from the diffraction pattern. Intermediate phases are not identified. It is clearer to identify the alumina peaks in microcomposites than nanocomposites. This may be due to the larger size and higher volume fraction of the microcomposites.

4.1.2 SEM

4.1.2.1 Nanocomposite

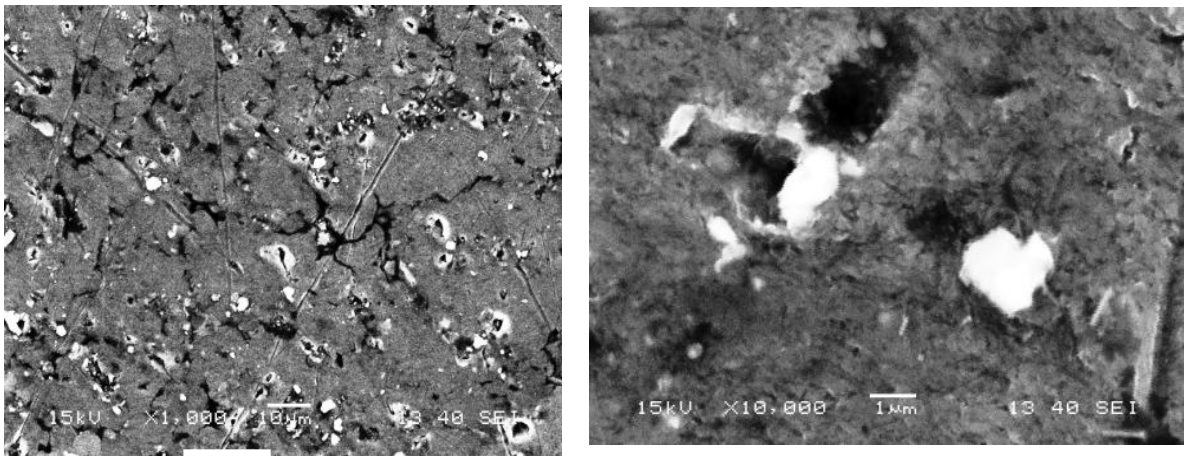

(a) (b)

Fig. 4.3 (a) and (b) showing the SEM micrographs of as-fabricated 1 vol. % nanocomposite.

The SEM micrographs of the as-fabricated 1 vol. % nanocomposite taken in secondary electron mode are shown in the fig. 4.3 (a) & (b). From the fig. 4.3 (a), it is seen that the distribution of nano alumina particles in the aluminium matrix is very uniform. Voids are also visible at certain regions. The failure process of particle pullout is observed in the fig. 4.3 (b). This suggests weak bonding between the particles and the matrix.

4.1.2.2 Microcomposite

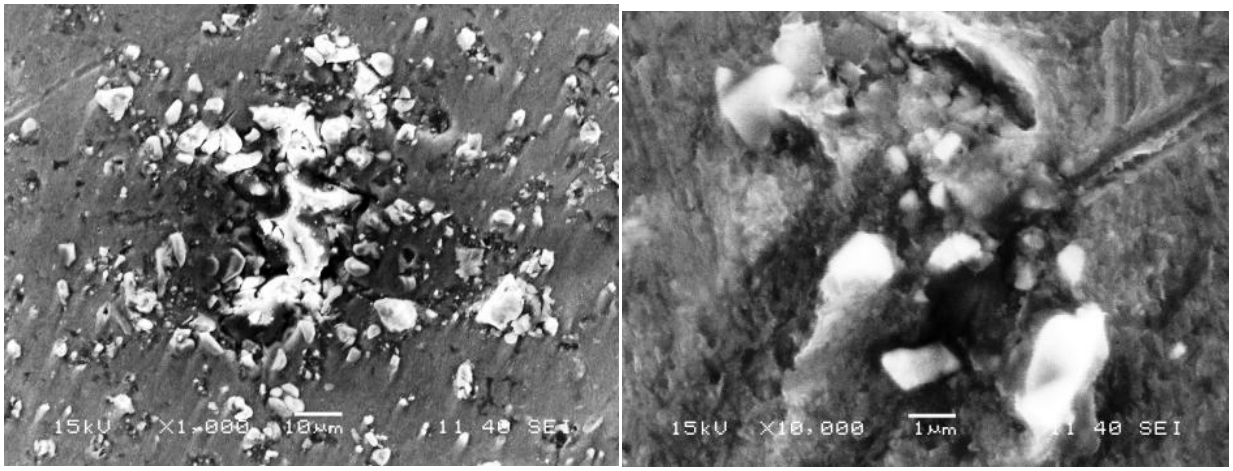

(a) (b)

Fig. 4.4 (a) and (b) showing the SEM micrographs of as-fabricated 5 vol. % microcomposite.

Particle clustering was observed in the SEM micrograph of as-fabricated 5 vol. % microcomposite depicted in the fig. 4.4 (a). The particles here have a random distribution compared to the nanocomposite. Presence of voids is also visible. Interfacial integrity is also weak here showing the traces of interfacial decohesion in fig. 4.4 (b).

4.2 Physical property analysis

4.2.1 Density measurement

Composition	Sintered density (g/cc)	% of theoretical density
5 vol. % nanocomposite	2.52	91.3
5 vol. % microcomposite	2.55	92.39

Table 4. 1 The density values of as-fabricated 5 vol. % nano- and microcomposites.

Archimedes principle was employed to find out the density of the composites. The theoretical density was determined using the rule of mixtures. The densities of the as-fabricated 5 vol. % nano- and microcomposite are displayed in table 4.1. The densities of the two are almost the same with nanocomposite showing slightly higher value. Lesser density of nanocomposite may be due to increase in void volume fraction.

4.3 Mechanical Testing

4.3.1 Micro-hardness test

Composition	Average micro-hardness value (HV)
5 vol. % nanocomposite	31.675
5 vol. % microcomposite	35.775

Table 4. 2 Micro-hardness values of as-fabricated 5 vol. % nano- and microcomposites.

The mean Vickers micro-hardness values of as-fabricated 5 vol. % nano- and micro-composites are shown in table 4.2. It is seen that the average micro-hardness value of 5 vol. % microcomposite is higher than that of nanocomposite. Since the interfacial area of nanocomposites is more, effects of interfacial decohesion and particle pullout (as observed from

SEM micrograph in fig. 4.3 (b)) is also greater. This will lead to decrement in their micro-hardness values.

4.3.1.1 Air cooling

4.3.1.1.1 Nanocomposite

Composition (%)	Avg. micro-hardness before quenching		Avg. micro-hardness after quenching		Percentage change in micro-hardness value (%)	
	200°C	300°C	200°C	300°C	200°C	300°C
1	47.9	31.15	45.125	42.15	-5.79332	35.31
3	45.075	47.625	44.45	44.175	-1.38656	-7.24409
5	39.45	36	44.825	42.175	13.62484	17.15278
7	31.425	38.425	43.025	40.9	36.91329	6.44112

Table 4. 3 Micro-hardness values of air cooled nanocomposites

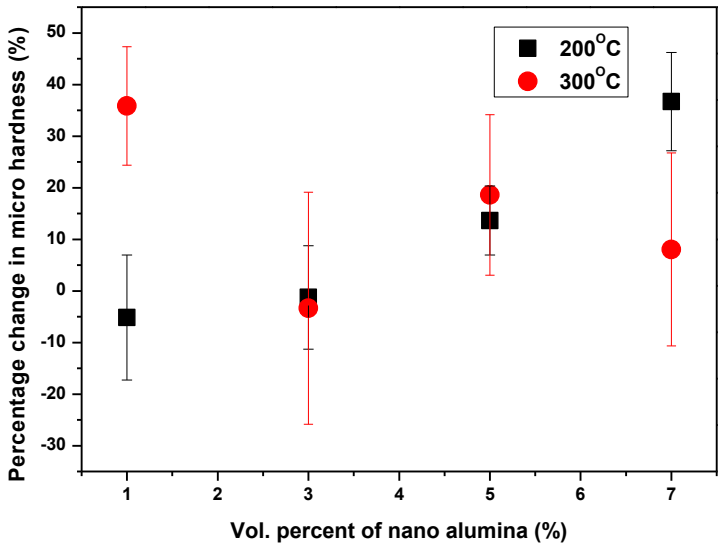

Fig. 4.5 Plot of % change in micro-hardness vs vol. % of nano alumina for air cooled samples.

The mico-hardness values of Al-Al_2O_3 nanocomposites after quenching were observed to be increasing with increasing volume fraction of particles at conditioning temperature of 200°C, whereas they tend to decrease with increasing particle content for conditioning temperature of

300°C. The improvement in micro-hardness is less as a result of low cooling rate which inturn results in less dislocation density. The increase in dislocation density arising due to CTE mismatch between the matrix and the reinforcement is an important factor which enhances the hardness of composites. Due to slow cooling from quenching temperature, there is a higher tendency for grain coarsening to occur. This imparts a good ductility but mediocre hardness. The drastic increment in micro-hardness values after quenching for 7 vol. % (at 200°C) and 1 vol. % (at 300°C) nanocomposites can be attributed to the hardening resulting from orowan bowing mechanism and good physical bonding at the interface as the matrix expands and exerts a compressive stress on the particles. The decrement in micro-hardness after quenching from 200°C for 1 and 3 vol. % nanocomposites may be due to increase in porosity. The higher agglomeration tendency of nanocomposites when temperature is increased to 300°C explains the decreased value of micro-hardness after quenching for 3 vol. % nanocomposite.

4.3.1.1.2 Microcomposite

Composition (%)	Avg. micro-hardness before quenching		Avg. micro-hardness after quenching		Percentage change in micro-hardness value (%)	
	200°C	300°C	200°C	300°C	200°C	300°C
5	36.15	34.85	35.15	37.2	-2.76625	7.98258
10	41.875	43.45	44.05	42.425	5.19403	-2.35903
15	48.025	41.9	47.8	40.2	-0.46851	-4.05728
20	49.675	39.85	50.775	50.425	2.21439	26.53701

Table 4. 4 Micro-hardness values of air cooled microcomposites

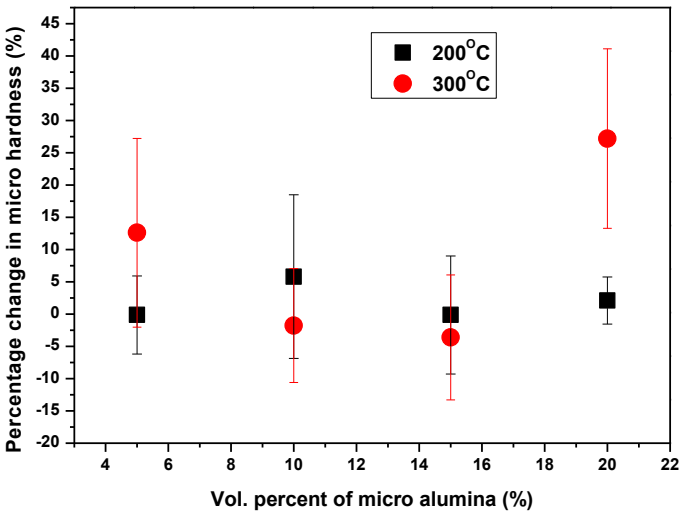

Fig. 4.6 Plot of % change in micro-hardness vs vol. % of micro alumina for air cooled samples.

For microcomposites quenched at 200°C, there was no significant improvement in micro-hardness values. The micro-hardness values were decreasing with increasing in particle content. The cooling rate was low enough to generate substantial amount of plastic flow in the matrix. When quenching temperature was increased to 300°C, drastic improvement was seen in the micro-hardness values with 20 vol. % microcomposite showing increase of 26.54% after quenching. This is due to higher number of hard alumina particles offering resistance to indentation and also as a result of better physical bonding at the interface when subjected to high temperature. Also, more number of dislocations are generated at higher temperature and their interaction with particles is also high. The agglomeration tendency is also less for microcomposites when compared to nanocomposites. The reduction in hardness values after quenching observed for some compositions is because of the porosity effect and matrix grain coarsening at higher temperature.

4.3.1.2 Brine water (7 wt. %) quenching

4.3.1.2.1 Nanocomposite

Composition (%)	Avg. micro-hardness before quenching		Avg. micro-hardness after quenching		Percentage change in micro-hardness value (%)	
	200°C	300°C	200°C	300°C	200°C	300°C
1	56.45	36.575	66.2	45.25	17.27192	23.71839
3	59.3	40.175	66	40.525	11.29848	0.87119
5	45.325	43.5	62.575	49.475	38.05847	12.8
7	56.95	42.375	60.9	46.7	6.93591	10.20649

Table 4. 5 Micro-hardness values of brine water quenched nanocomposites

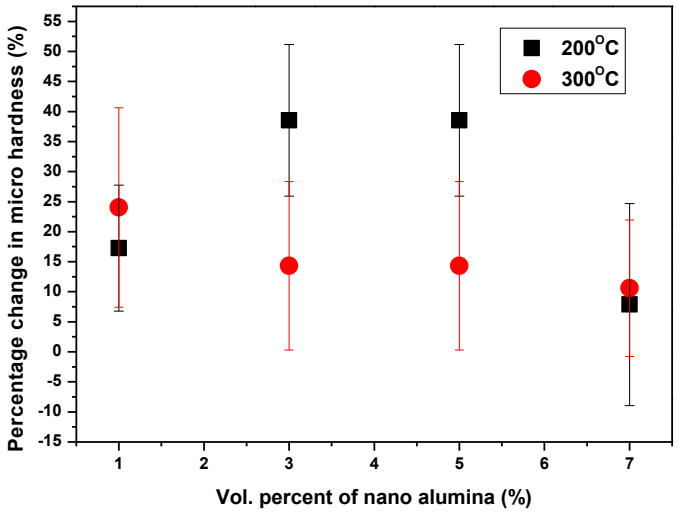

Fig. 4.7 Plot of % change in micro-hardness vs vol. % of nano alumina for brine quenched samples.

Significant enhancement in micro-hardness values were achieved as a result of brine quenching. This can be attributed to high density of dislocation formed due to the CTE mismatch between the matrix and the reinforcement. The cooling rate during brine quenching is high due to its low latent heat of vapourisation. i.e. it can be converted to vapour easily which inturn reduces the

vapour blanket stage of quenching. High cooling rate significantly improves the dislocation density. More interaction between the nanoparticle and the dislocations facilitates orowan strengthening effect. Also substantial grain refinement takes place due to effective pinning of dislocations by the nanoparticles at the grain boundaries, thereby inhibiting grain growth. Improvement in the micro-hardness values occurred with the addition of nanoparticles at quenching temperature of 200°C. The reduction in micro-hardness for 7 vol. % composition at 200°C may be either due to agglomeration of particles or enhancement in interfacial damage due to sudden contraction, resulting into pore formation. At 300°C , reduction in micro-hardness values with increasing volume fraction of particles was noticed which can be ascribed to enhanced agglomeration tendency for nanoparticles at higher temperatures.

4.3.1.2.2 Microcomposite

Composition (%)	Avg. micro-hardness before quenching		Avg. micro-hardness after quenching		Percentage change in micro-hardness value (%)	
	200°C	300°C	200°C	300°C	200°C	300°C
5	54.325	33.925	75.5	41.4	38.97837	22.0339
10	57.55	36.475	52.05	46.05	-9.55691	26.25086
15	44.875	37.875	44.825	43.025	-0.11142	13.59736
20	41.3	44.35	26.8	46.175	-35.10896	29.98873

Table 4. 6 Micro-hardness values of brine water quenched microcomposites

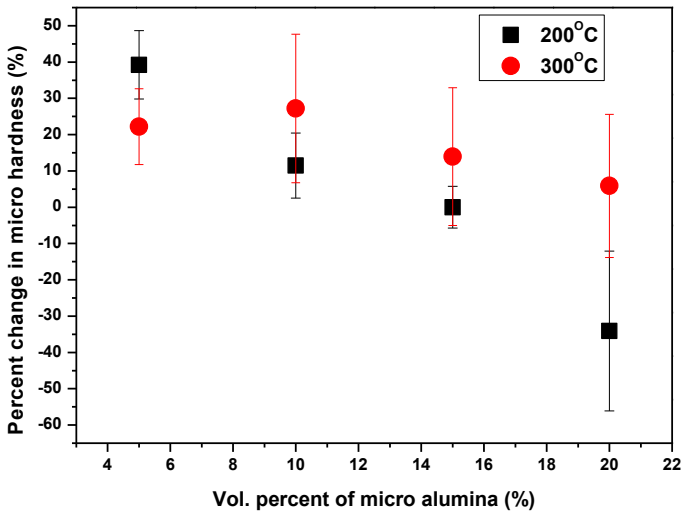

Fig. 4.8 Plot of % change in micro-hardness vs vol. % of micro alumina for brine quenched samples.

Brine quenching of microcomposites at 200°C showed high micro-hardness value of 75.5 HV for 5 vol. % composition. But, thereafter with increasing volume fraction of particles, micro-hardness values were observed to be declining. The reason may be due to increased microporosity formation with addition of microparticles. Increasing microporosity can create discontinuity in the matrix phase and thus enhance the formation of stress concentration points. Resistance to plastic deformation provided by the back stress effect created when the micro particles obstruct the dislocation movement is the prominent strengthening mechanism operating in microcomposites. Very low value of micro-hardness observed for 20 vol. % composition at 200°C might be due to distortion and cracking taking place in the sample surface as a result of high residual stress development. When quenching temperature is increased to 300°C, elevation in micro-hardness values were observed with increasing volume fraction of particles. The flow stress and dislocation density increases with increasing heat treatment temperature. Also physical bonding between particles and the matrix is high at elevated temperatures for microcomposites.

4.3.1.3 Oil quenching

4.3.1.3.1 Nanocomposite

Composition (%)	Avg. micro-hardness before quenching		Avg. micro-hardness after quenching		Percentage change in micro-hardness value (%)	
	200°C	300°C	200°C	300°C	200°C	300°C
1	40.3	35.775	40.175	41.5	-0.31017	16.0028
3	47.65	33.55	38.7	38.9	-18.78279	15.94635
5	48.525	38.775	42.4	40.4	-12.62236	4.19084
7	45.725	36.85	50.9	42.175	11.31766	14.45047

Table 4. 7 Micro-hardness values of oil quenched nanocomposites

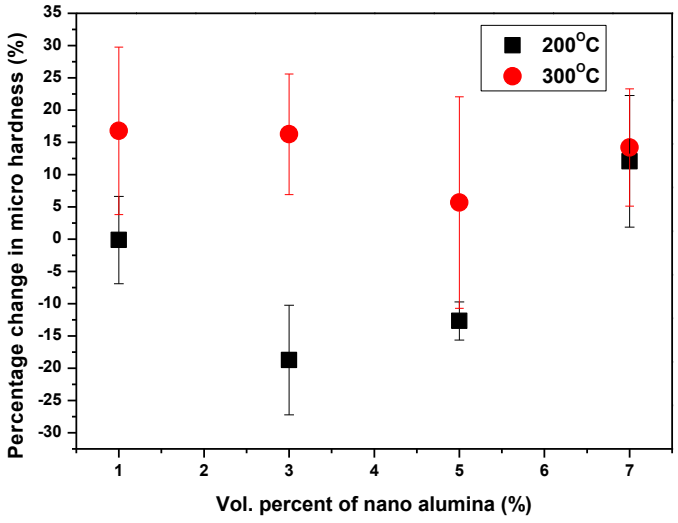

Fig. 4.9 Plot of % change in micro-hardness vs vol. % of nano alumina for oil quenched samples.

For oil quenching from 200°C temperature, improvement in micro-hardness value was observed only for 7 vol. % nanocomposite. The decrease in micro-hardness after quenching may be due to weak interfacial bonding between the nanoparticels and the aluminium matrix. Due to high viscosity of oil, vapour blanket stage gets prolonged resulting in low cooling rate. This significantly reduces the dislocation density formation due to CTE mismatch. As quenching temperature is increased to 300°C, there is substantial improvement in micro-hardness values. This is due to lowering of viscosity of oil at higher temperature resulting in enhanced cooling

rate. With increasing volume fraction of particles, there is slight decrement in the percentage change in micro-hardness values. But for 5 vol. % nanocomposite, increase in micro-hardness value is comparitively lower which might be due to agglomeration tendency of nanoparticles at higher temperatures.

4.3.1.3.2 Microcomposite

Composition (%)	Avg. micro-hardness before quenching		Avg. micro-hardness after quenching		Percentage change in micro-hardness value (%)	
	200°C	300°C	200°C	300°C	200°C	300°C
5	42.325	37.4	41.55	39	-1.83107	4.27807
10	39.225	40.825	39.85	41.325	1.59337	1.22474
15	32.95	46.35	32.475	48.375	-1.44158	4.36893
20	37.075	38.95	38.075	43.7	2.69724	12.19512

Table 4. 8 Micro-hardness values of oil quenched microcomposites

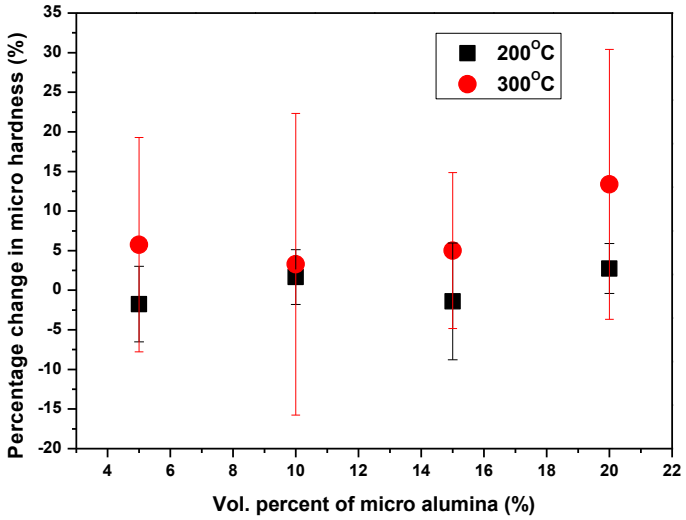

Fig. 4.10 Plot of % change in micro-hardness vs vol. % of micro alumina for oil quenched samples.

Oil quenched microcomposites only projected marginal increase in the micro-hardness values with increasing volume fraction of the particles. This can be due to lesser back stress effect of

particles resulting from lower dislocation density. So resistance for indentation is less. The high latent heat of vapourisation of oil also results in its lower cooling potential. When temperature is increased to 300°C, micro-hardness values were found to be increasing with increasing volume fraction of particles. The viscosity of oil is reduced at higher temperature and thus quenching effect is enhanced. More dislocations are generated which are obstructed by the micro-particles creating more back stress effect.

4.3.1.4 Liquid nitrogen quenching

4.3.1.4.1 Nanocomposite

Composition (%)	Avg. micro-hardness before quenching		Avg. micro-hardness after quenching		Percentage change in micro-hardness value (%)	
	200°C	300°C	200°C	300°C	200°C	300°C
1	40.575	37.825	47.55	40.1	17.19039	6.01454
3	47.55	37.8	52.75	45.925	10.93586	21.49471
5	53	36.6	65.2	43.225	23.01887	18.10109
7	57.975	37.875	63.225	41.7	9.05563	10.09901

Table 4. 9 Micro-hardness values of liquid nitrogen quenched nanocomposites

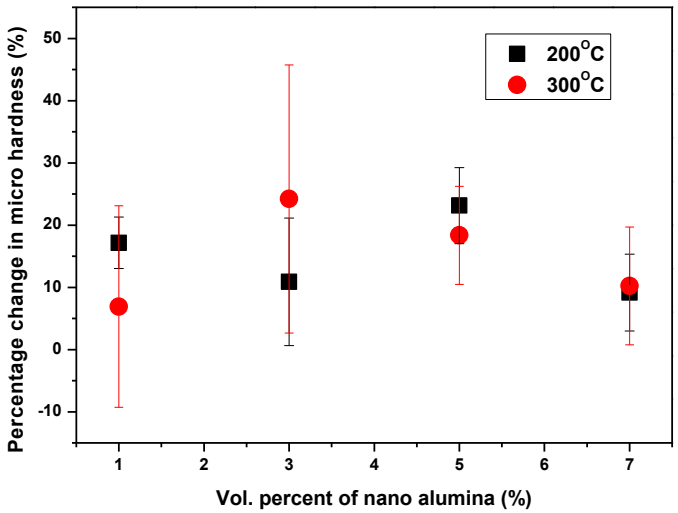

Fig. 4.11 Plot of % change in micro-hardness vs vol. % of nano alumina for liquid nitrogen quenched samples.

Enhancement in micro-hardness values was found for liquid nitrogen quenched nanocomposites which can be attributed to the brittleness induced due to high cooling power of liquid nitrogen. The temperature gradient is very high during liquid nitrogen quenching which results in enhanced dislocation forest formation due to CTE mismatch. Also matrix grain refinement will be more due to efficient pinning of nanoparticles at the grain boundaries. The increase-decrease trend of micro-hardness with volume fraction of reinforcements was found for both quenching temperature of 200°C and 300°C. The decrease in micro-hardness with increasing volume fraction of nanoparticles may be due to increased tendency for interfacial damage as residual stresses developed are more. These residual stresses are not able to relax at low cryogenic liquid nitrogen temperature (-196°C) which inturn will lead to high chances of interfacial decohesion to occur. Also sudden contraction during liquid nitrogen quenching causes distortion and debonding at the interface.

4.3.1.4.2 Microcomposite

Composition (%)	Avg. micro-hardness before quenching		Avg. micro-hardness after quenching		Percentage change in micro-hardness value (%)	
	200°C	300°C	200°C	300°C	200°C	300°C
5	33.625	34.95	43.175	42.675	28.40149	22.103
10	32.5	36.3	47.675	45.825	46.69231	26.23967
15	34.425	36.4	53.35	49.675	54.97458	36.46978
20	34.425	38.625	54.3	50.425	57.7342	30.55016

Table 4. 10 Micro-hardness values of liquid nitrogen quenched microcomposites

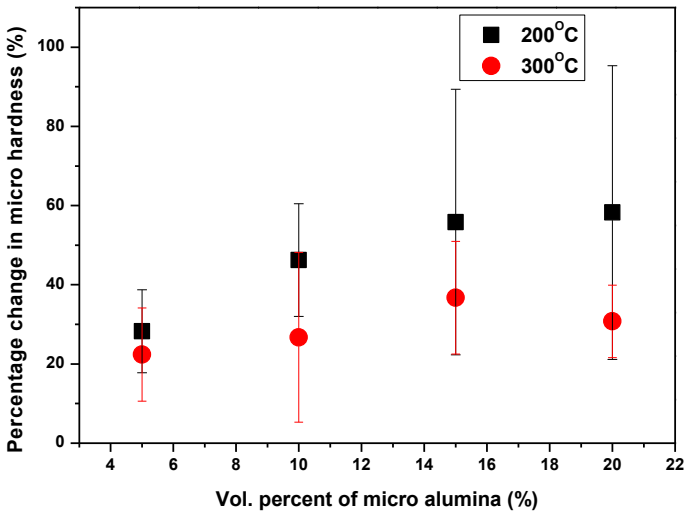

Fig. 4.12 Plot of % change in micro-hardness vs vol. % of micro alumina for liquid nitrogen quenched samples.

Superior improvement in micro-hardness values with increasing particle volume fraction was observed for microcomposites during liquid nitrogen quenching at both 200°C and 300°C temperature. This can be ascribed to the high brittleness induced in the composite due to very high temperature gradient of heat treatment. High back stress is developed due to particles blocking the movement of dislocations. This along with the possible presence of quenched-in vacancies and dislocation jogs which can increase the yield strength further elevates the micro-hardness values. The improvement in micro-hardness at 300°C quenching temperature is less compared to 200°C temperature because of the chances of distortion and particle cracking due to high thermal residual stress development.

4.3.1.5 Polymer (5 vol. %PEG) quenching

4.3.1.5.1 Nanocomposite

Composition (%)	Avg. micro-hardness before quenching		Avg. micro-hardness after quenching		Percentage change in micro-hardness value (%)	
	200°C	300°C	200°C	300°C	200°C	300°C
1	40.625	37.625	40.075	42.7	-1.35385	13.48837
3	42.4	34.525	43.95	47.75	3.65566	38.30558
5	39.975	37.7	45.15	41.825	12.94559	10.94164
7	39.875	40.05	43.75	44.1	9.71787	10.11236

Table 4. 11 Micro-hardness values of polymer quenched nanocomposites

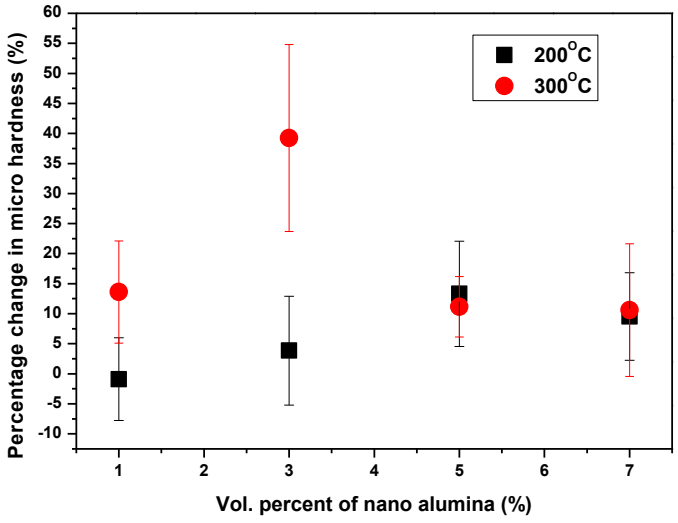

Fig. 4.13 Plot of % change in micro-hardness vs vol. % of nano alumina for polymer quenched samples.

For polymer quenching, an increase-decrease trend was found for micro-hardness values for both conditioninig temperatures of 200°C and 300°C temperature. Polymer quenching has the peculiar property of inverse solubility by which a thin film of glycol is formed around to wet the work piece as it is quenched, which can suppress the formation of vapour blanket stage, thereby increasing the cooling rate. When temperature of work piece lowers down this thin film dissolves and permits fast removal of heat from it. Higher the quenching temperature, more faster the

dissolving of the glycol film and the heat transfer rate. The high increase in micro-hardness for quenching at 300°C can be attributed to increased nano-particle interaction with the dislocations produced as a result of CTE mismatch. The reduction in micro-hardness values for higher volume fractions at both temperatures can be due to the agglomeration tendency of nanoparticles. During agglomeration, the interparticle spacing is increased which provides easy movement of dislocations and thus lower hardening effect. Superior improvement in micro-hardness was seen for 3 vol. % nanocomposite at 300°C conditioning temperature.

4.3.1.5.2 Microcomposite

Composition (%)	Avg. micro-hardness before quenching		Avg. micro-hardness after quenching		Percentage change in micro-hardness value (%)	
	200°C	300°C	200°C	300°C	200°C	300°C
5	46.15	32.35	42.95	40.525	-6.93391	25.27048
10	36.875	37.425	36.625	49.325	-0.67797	31.79693
15	57.525	40.35	42	45.325	-26.98827	12.32962
20	39.875	39.15	40.725	46.225	2.13166	18.07152

Table 4. 12 Micro-hardness values of polymer quenched microcomposites

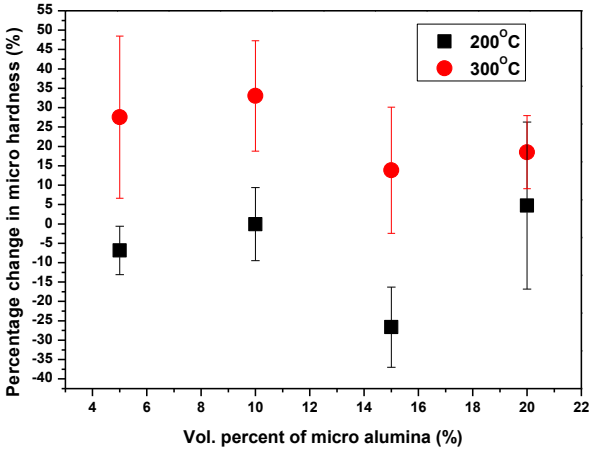

Fig. 4.14 Plot of % change in micro-hardness vs vol. % of micro alumina for polymer quenched samples.

In the case of microcomposites, decrease in micro-hardness after quenching from 200°C was observed for upto 15 vol. % of particles. This is due to slow cooling rate resulting from high specific heat of the polymer medium. The temperature is not sufficient enough to dissolve the glycol film formed over the surface. This increases the duration of vapour blanket stage which inturn creates time for high degree of dislocation annihilation and plastic deformation to take place. Also, micro-porosity formation and interface damage accumulation will be high. At higher quenching temperature of 300°C, more dislocations are generated after quenching due to higher temperature gradient. Also, the 300°C is sufficient enough to make the dissolution of thin glycol film faster, which permits faster cooling effect. At higher volume fractions of particle, the decrement in micro-hardness values may be due to inefficient bonding between the particles and the matrix.

4.3.2 3-point flexural test

4.3.2.1 Air cooling

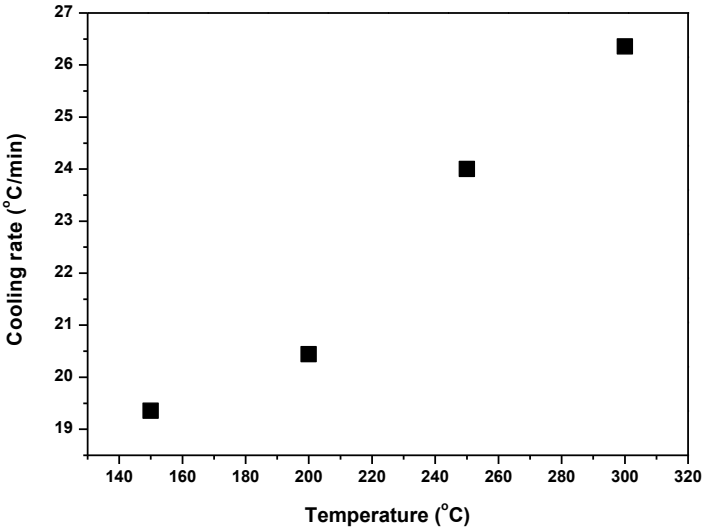

Fig. 4. 15 Plot showing the variation of cooling rate with conditioning temperature for air cooled specimens

The variation of cooling rate with quenching temperature for air cooled samples is as shown in Fig. 4.15. Cooling rate was observed to increase with increase in conditioning temperature from 150°C to 300°C.

4.3.2.1.1 Nanocomposite

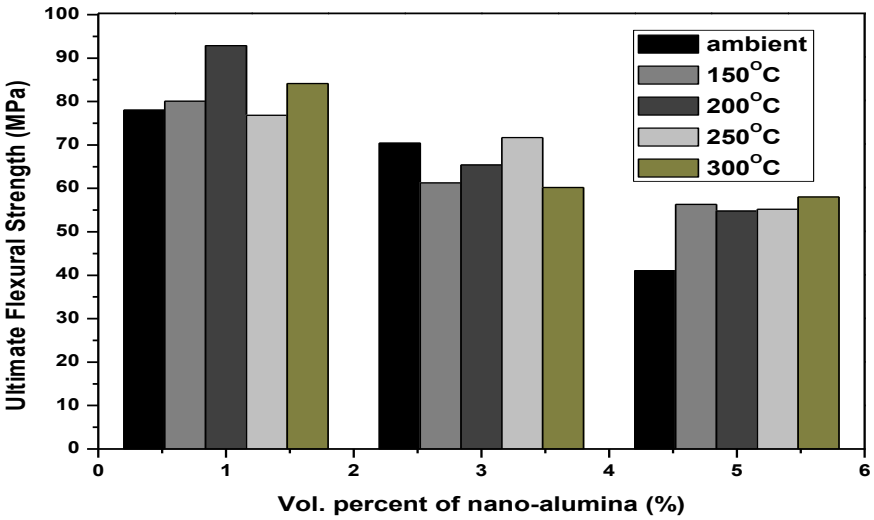

Fig. 4. 16 Plot showing the variation of ultimate flexural strength with vol. % of reinforcement for nanocomposite after air cooling.

Air cooling provided only marginal increase in flexural strength for nanocomposites when compared to their ambient values. This is due to low cooling rate which decreases with decreasing temperature of heat treatment. The heat transfer from the specimen to the surrounding air flow takes place mainly through convection process which is very slow. The dislocation density generated due to CTE misfit is less enough to initiate substantial nanoparticle-dislocation interactions which inturn results in less strengthening due to orowan mechanism. Increasing the nano particle content resulted in decrement of flexural strength at all temperatures. The large interfacial area presented by nano-particles makes it more prone to interfacial damage. Also, the agglomeration tendency is enhanced when more nanoparticles are present.

As the effect of conditioning temperature on flexural strength is more pronounced for lower vol. % of reinforcement, the variation of flexural strength with conditioning temperature is plotted for 1 vol. % nanocomposite in Fig. 4.17.

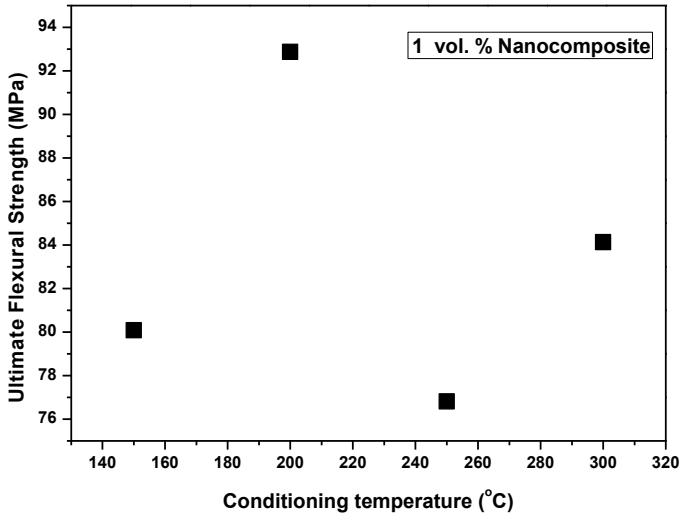

Fig. 4.17 Plot showing the variation of flexural strength with conditioning temperature for 1 vol. % nanocomposite after air cooling

The flexural strength of 1 vol. % nanocomposite showed an increase-decrease trend with elevation in conditioning temperature with maximum strength at temperature of 200°C. Provision of more time for various relaxational processes such as dislocation annihilation and plastic deformation to occur at higher temperatures can be used to explain the lowering of strength at 250°C.

4.3.2.1.2 Microcomposite

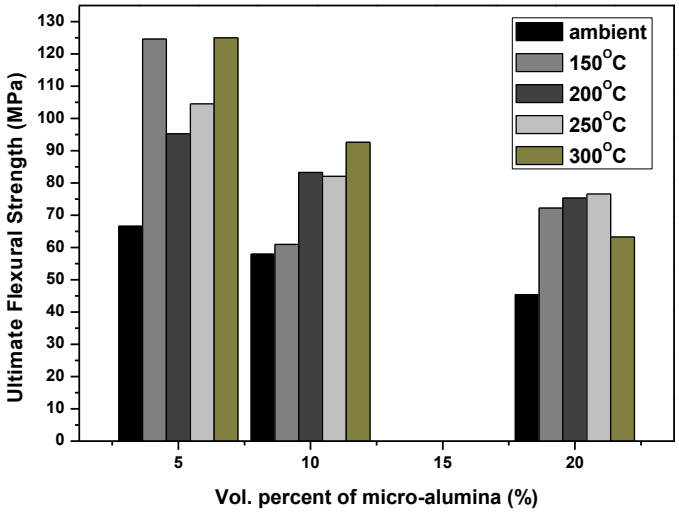

Fig. 4.18 Plot showing the variation of ultimate flexural strength with vol. % of reinforcement for microcomposite after air cooling

Contrary to the behavior of nanocomposites, the flexural strength of microcomposites showed appreciable improvement after air cooling. The reason may be due to piling up of dislocations in the particles which increases the stress concentration near it and initiates crack. Energy is absorbed when the hard particles discrete particles act to temporarily pin down the advancing crack front and deflects it through crack blunting mechanisms. This enhances the fracture toughness and strength of the composite. The flexural strength decreased with increasing volume fraction of the reinforcement at all conditioning temperatures. This may be due to increase in the number of damage accumulation zones as interfaces are more.

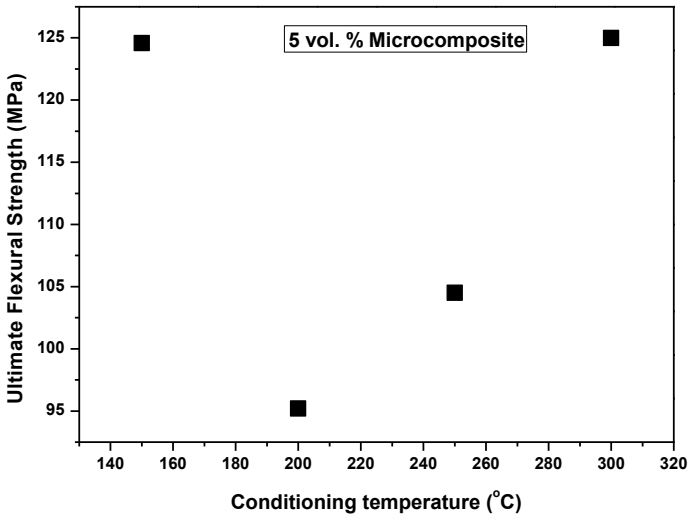

Fig. 4.19 Plot showing the variation of flexural strength with conditioning temperature for 5 vol. % microcomposite after air cooling

The higher cooling rate at conditioning temperature of 300°C reflects the enhancement in flexural strength as shown in fig. 4.19.

4.3.2.2 Brine water (7 wt. %) quenching

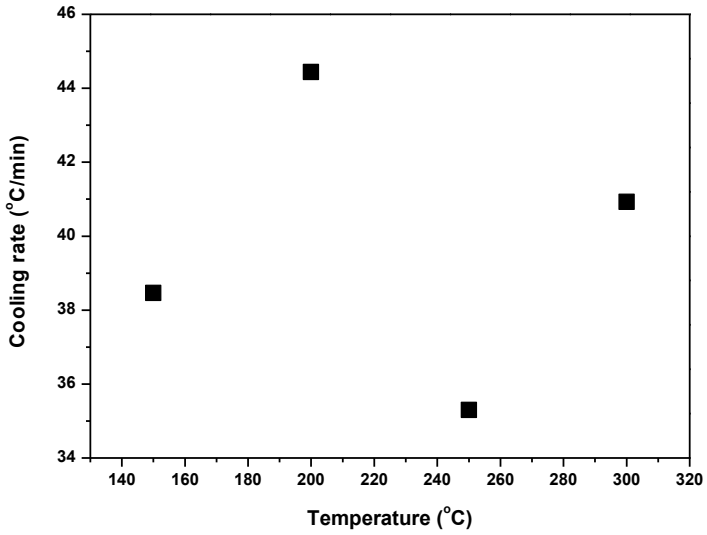

Fig. 4.20 Plot showing the variation of cooling rate with conditioning temperature for brine quenched specimens

The variation of cooling rate with quenching temperature for brine water quenched samples is as shown in Fig. 4.20. Cooling rate was observed to have an increase-decrease tendency with increasing conditioning temperature. The addition of NaCl to distilled water reduces its viscosity and thus decreases the formation of vapour blanket stage. This results in improved cooling capacity for brine solution.

4.3.2.2.1 Nanocomposite

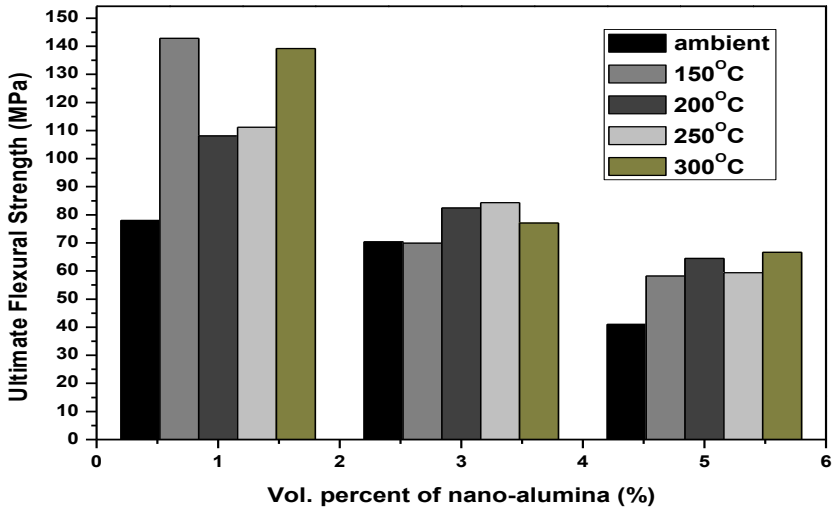

Fig. 4.21 Plot showing the variation of ultimate flexural strength with vol. % of reinforcement for nanocomposite after brine quenching

Brine quenching yielded higher strength to nanocomposites when compared with ambient test values. The higher cooling power of brine quenching enhances the dislocation generation due to CTE mismatch in the composite. The dislocations generated are sufficiently extensive to cover most of the matrix domain. The nano-particle dislocation interactions are enhanced due to this high dislocation density produced. The nano-particles pin down the grain boundaries, inhibiting grain growth and further enhancing the strength. The increasing dislocation density also accelerates the grain refining process. The flexural strength was observed to decrease with increasing volume fractions of particle which is ascribed to increasing tendency for agglomeration and interfacial damage.

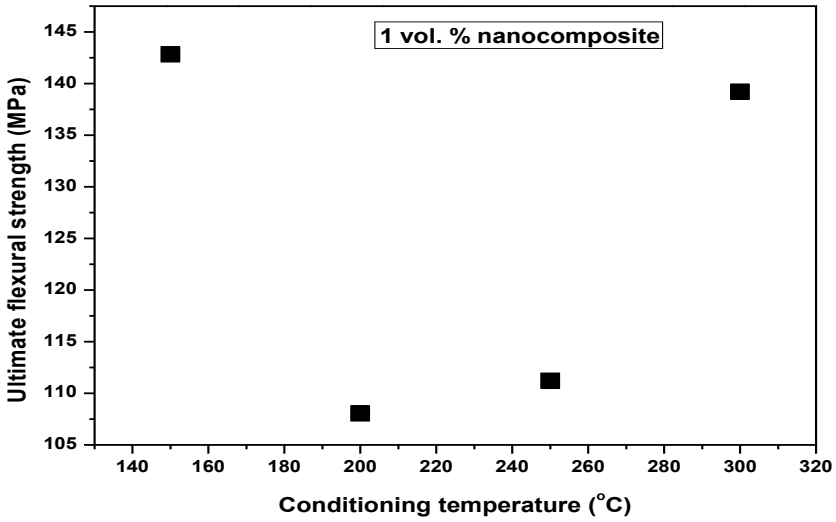

Fig. 4.22 Plot showing the variation of flexural strength with conditioning temperature for 1 vol. % nanocomposite after brine water quenching

The decrease in ultimate flexural strength with quenching temperature for 200°C temperature may be due to lower amount of dislocation density formed as a result of low cooling rate.

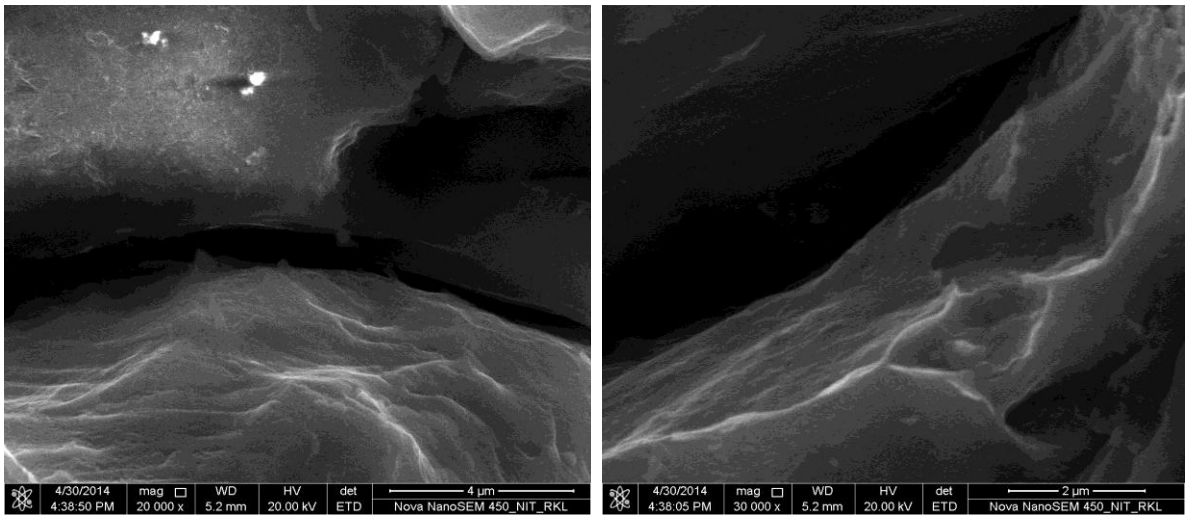

(a) (b)

Fig. 4.23 Fractography of 3-point bend test sample of 5 vol. % nanocomposite quenched in brine water from temperature of 300°C shown at (a) 20,000X and (b) 30,000X magnifications.

Flat fracture surfaces with tear ridges due to crack propagation was observed in the case of 5 vol. % nanocomposite quenched in brine water from temperature of 300°C. Riverline markings are also present in the fracture surface. Microcrack path can also be seen in the fractography images.

4.3.2.2.2 Microcomposite

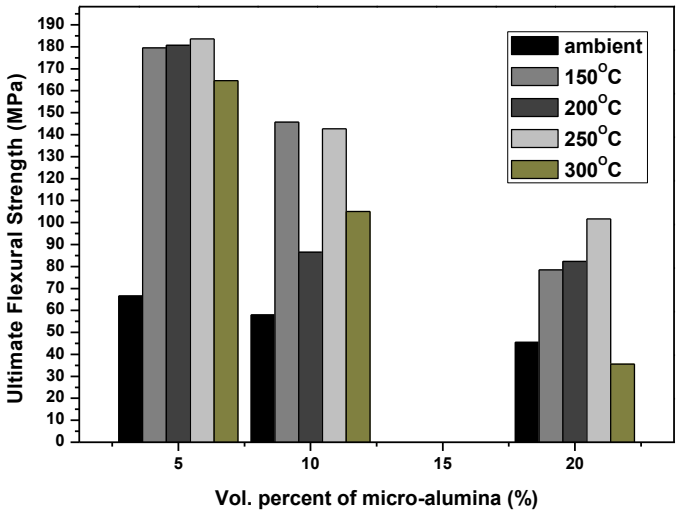

Fig. 4.24 Plot showing the variation of ultimate flexural strength with vol. % of reinforcement for microcomposite after brine quenching

Microcomposites displayed higher flexural strength than nanocomposites due to the combined effects of high dislocation density generation due to CTE mismatch, larger particle back stress effect and strengthening due to crack blunting mechanisms. The dislocation piling upon the particle enhances the stress intensity at the crack tip. Toughening due to deflection of the crack propagation path occurs. More strain energy will be needed for new crack surface formation according to Griffiths crack theory criterion. Thus both the fracture toughness and strength of the microcomposites are enhanced. The tendency for particle cracking is less for nanocomposites since they are more fine and hard, thus becoming impenetrable by dislocation. Dislocations cannot cut through them and are only allowed to bow or bend around them (Orowan strengthening). At higher volume fractions, flexural strength got reduced which may be due to enhanced clustered regions where crack propagation is easier.

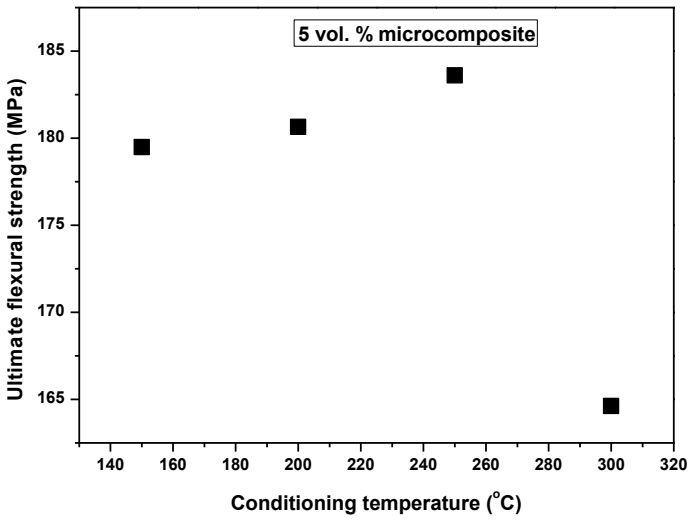

Fig. 4.25 Plot showing the variation of flexural strength with conditioning temperature for 5 vol. % microcomposite after brine water quenching

The ultimate flexural strength of 5 vol. % microcomposites depicted a sudden decrement at temperature of 300°C which may be due to increasing tendency for matrix grain coarsening and dislocation annihilation at higher thermal regimes.

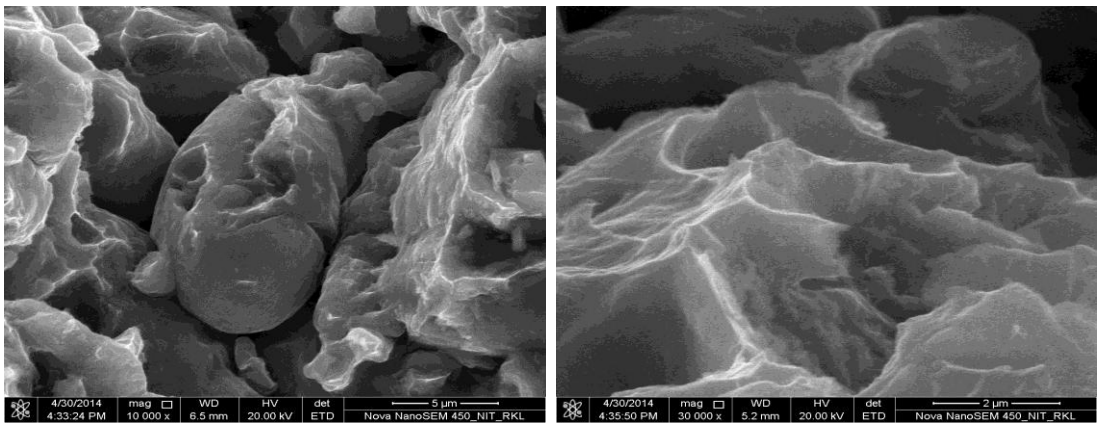

(a) (b)

Fig. 4.26 Fractography of 3-point bend test sample of 5 vol. % microcomposite quenched in brine water from temperature of 300°C shown at (a) 10,000X and (b) 30,000X magnifications.

Fractographs of 5 vol. % microcomposite quenched in brine water shows evidence of tear ridges present. The occurrence of dimples as depicted in fig. 4.26 (b) is an evidence of ductile failure.

4.3.2.3 Oil quenching

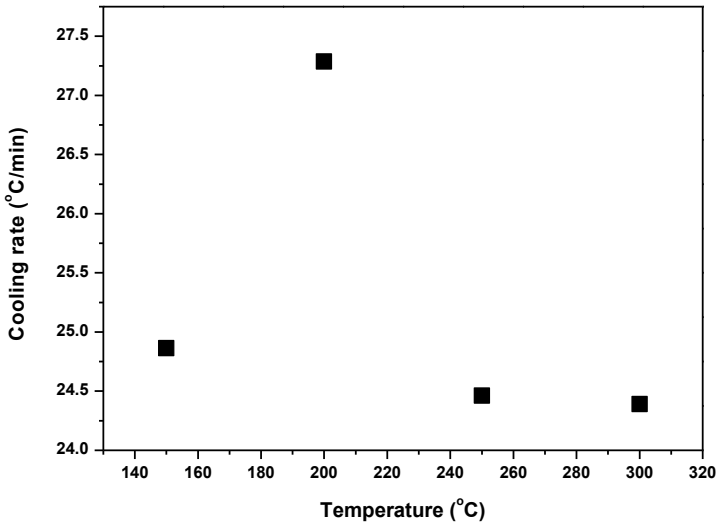

Fig. 4.27 Plot showing the variation of cooling rate with conditioning temperature for oil quenched specimens

Oil quenched specimens showed an initial increase in cooling rate with conditioning temperature upto 200°C, thereafter declining at higher temperatures. Since the viscosity of oil reduces at higher temperatures, ideally the cooling rate should increase with higher quenching temperature. But, here the declining of cooling rate at higher temperatures may be due to lowering of heat transfer coefficient (h) which has also a profound influence on determining the cooling rate.

4.3.2.3.1 Nanocomposite

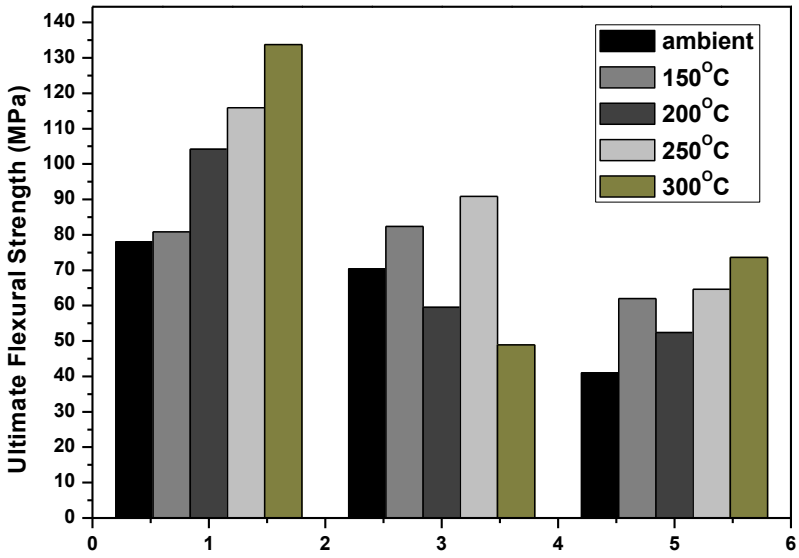

Fig. 4.28 Plot showing the variation of ultimate flexural strength with vol. % of reinforcement for nanocomposite after oil quenching

Oil quenched samples also depicted improvement in flexural strength for nanocomposites from the ambient values. Due to low cooling rate of oil by virtue of its low viscosity, the dislocation densities produced are less when compared with brine water quenching. Also the high latent heat of vapourisation of oil permits less heat transfer rate. So, nanoparticle-thermal misfit dislocation interactions are reduced here. Oil quenching provides less distortion and cracking than other quenchants despite its low cooling potential. Oil quenching also follows the trend of decline in flexural strength for higher particle volume fractions which may due to increase in interface damage accumulation zones.

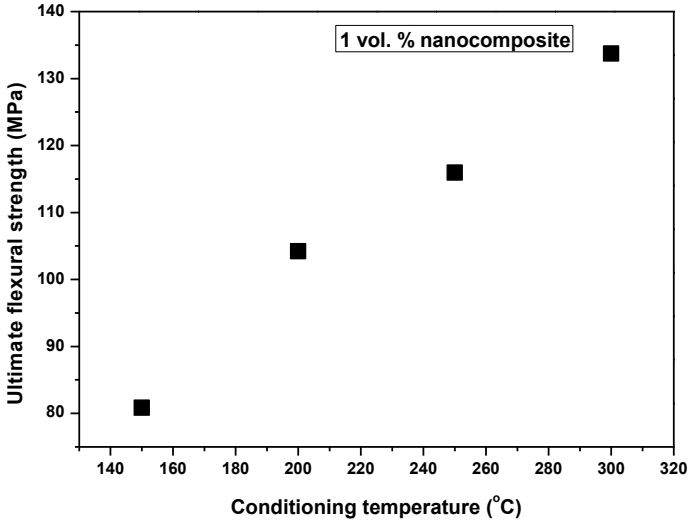

Fig. 4.29 Plot showing the variation of flexural strength with conditioning temperature for 1 vol. % nanocomposite after oil quenching

Fig. 4.29 depicts increase in flexural strength with increasing conditioning temperature. This can be attributed to the lowering of the viscosity of oil as temperature increases, which results in faster cooling rate and thus high dislocation density generation.

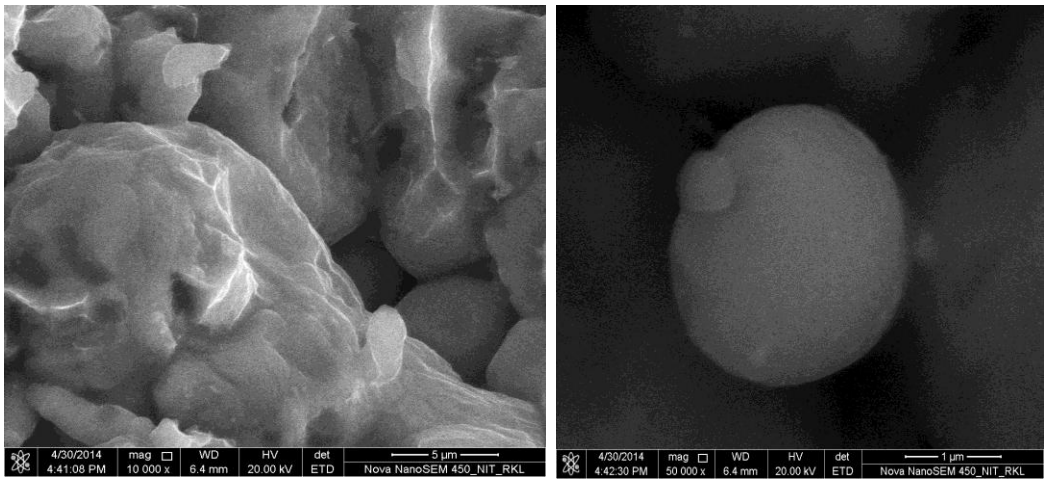

(a) (b)

Fig. 4.30 Fractography of 3-point bend test sample of 5 vol. % nanocomposite quenched in oil from temperature of 300°C shown at (a) 10,000X and (b) 50,000X magnifications.

4.3.2.3.2 Microcomposite

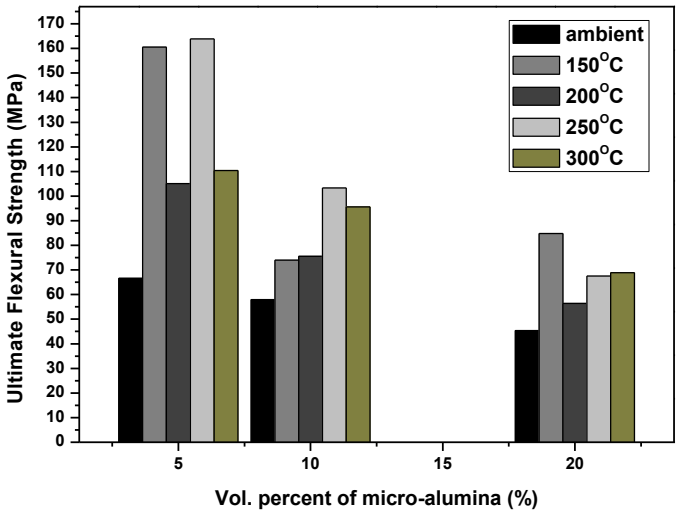

Fig. 4.31 Plot showing the variation of ultimate flexural strength with vol. % of reinforcement for microcomposite after oil quenching

Microcomposites displayed higher elevation in flexural strength than nanocomposites due to additional toughening mechanism resulting from crack blunting mechanisms. The matrix plasticity around the cracked particle plays an important role in this toughening mechanism. Also the back stress effect of particles obstructing the dislocation motion further enhances the flexural strength. With increasing particle volume fraction, strength comes down as seen for all the other cases.

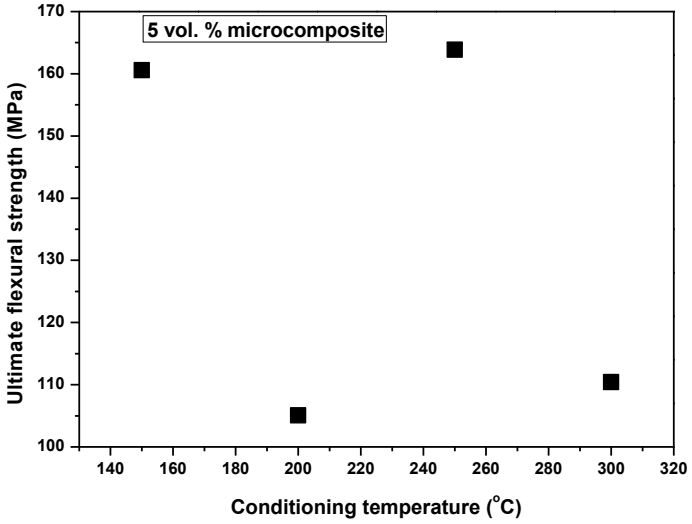

Fig. 4.32 Plot showing the variation of flexural strength with conditioning temperature for 5 vol. % microcomposite after oil quenching

The flexural strength showcased a decrease-increase trend with conditioning temperature as shown in fig. 4.32. The decrement of strength with temperature might be due to lowering of heat transfer coefficient whereas increase in flexural strength with temperature is due to decreasing viscosity of oil providing high cooling rate.

4.3.2.4 Liquid nitrogen quenching

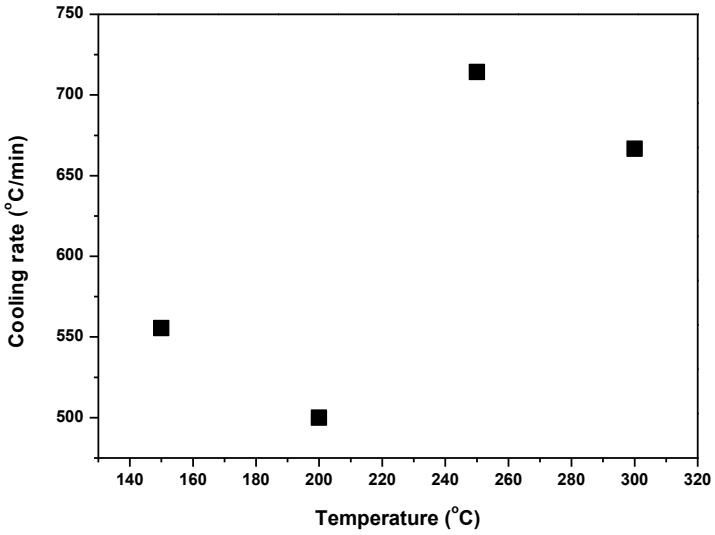

Fig. 4.33 Plot showing the variation of cooling rate with conditioning temperature for liquid nitrogen quenched specimens

The cooling rates of liquid nitrogen quenching are stupendously high as compared to other quenchants. The variation of cooling rate with quenching temperature moreover depicted an increasing trend reaching very high cooling rates above 700°C/minute.

4.3.2.4.1 Nanocomposite

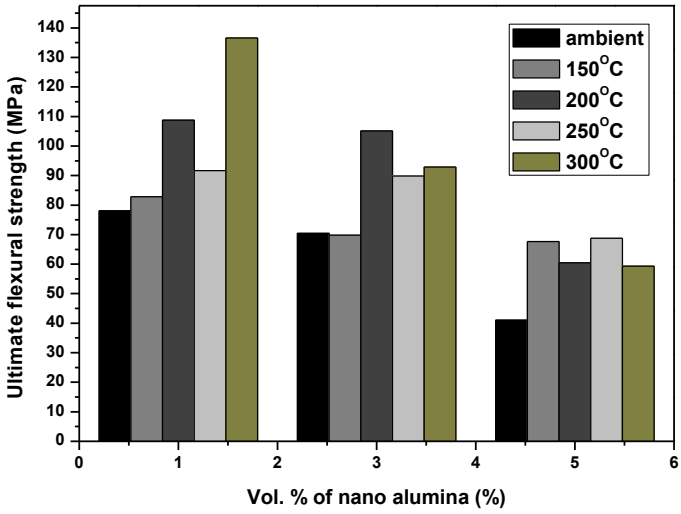

Fig. 4.34 Plot showing the variation of ultimate flexural strength with vol. % of reinforcement for nanocomposite after liquid nitrogen quenching

Liquid nitrogen quenching resulted in elevation of flexural strength for nanocomposites due to the high degree of brittleness induced due to quenching from a very high temperature gradient. The liquid nitrogen provides sudden cooling leading to more tangling of dislocations and formation of dislocation forest. Eventhough the cooling rate and hence dislocation forming capacity of liquid nitrogen is very high, the flexural strength was observed to be less than brine and oil quenchants which have relatively very low cooling rates. The can be explained in terms of higher dislocation interaction and annihilation occurring, when more dislocations are present. The orowan nanoparticle dislocation interaction also operates leading to enhancement in strength.

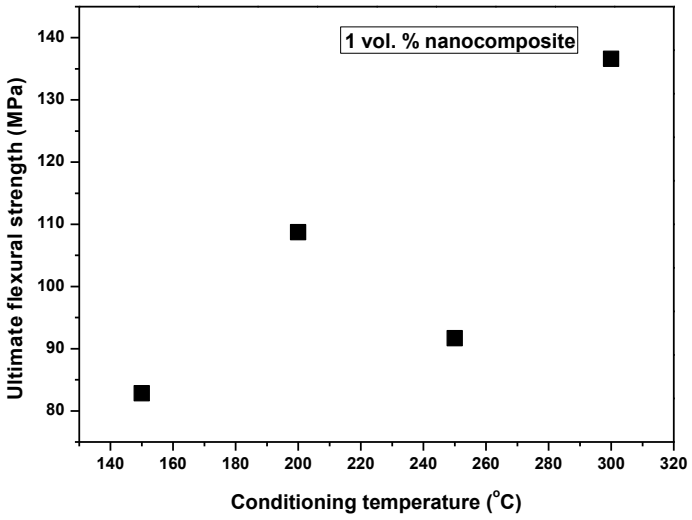

Fig. 4.35 Plot showing the variation of flexural strength with conditioning temperature for 1 vol. % nanocomposite after liquid nitrogen quenching

The flexural strength for 1 vol. % nanocomposite showed an increasing trend with conditioning temperature. Formation of quenched –in vacancies and dislocation jogs can elevate the yield strength of particle reinforced composites during liquid nitrogen quenching. As temperature is more, vacancy generation will also be more. This results in enhanced strengthening effect with increase in temperature. Brittle mode of failure can be seen for nanocomposite quenched in liquid nitrogen from the fig. 4.36. The fracture surfaces are flat and faceted in nature.

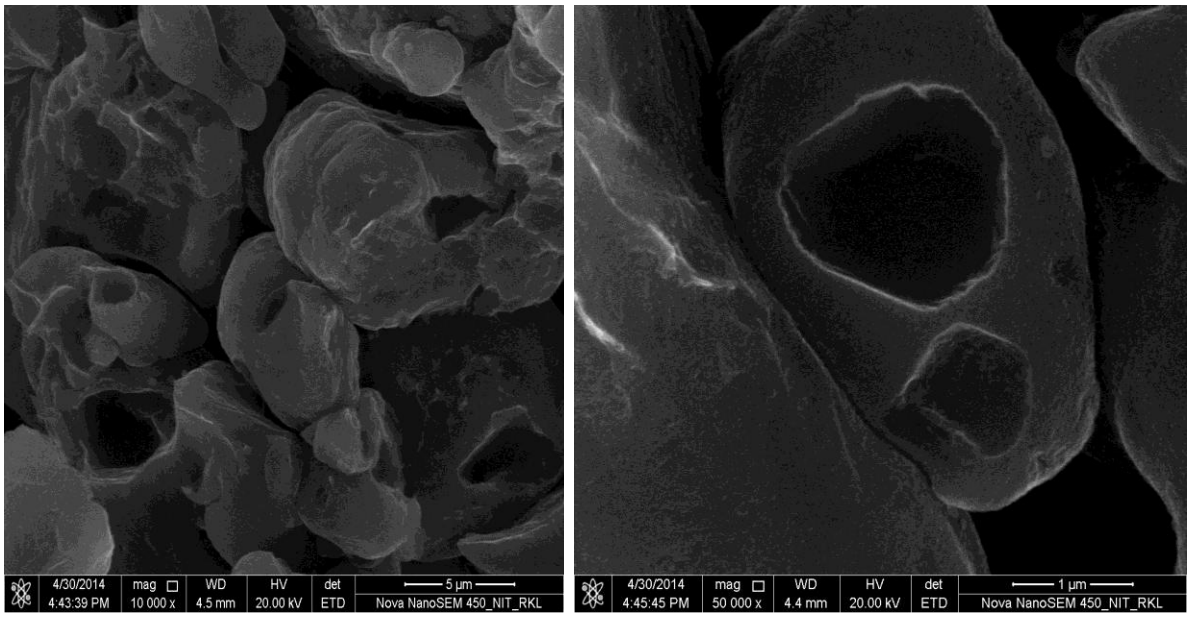

(a) (b)

Fig. 4.36 Fractography of 3-point bend test sample of 5 vol. % nanocomposite quenched in liquid nitrogen from temperature of 300°C shown at (a) 10,000X and (b) 50,000X magnifications.

4.3.2.4.2 Microcomposite

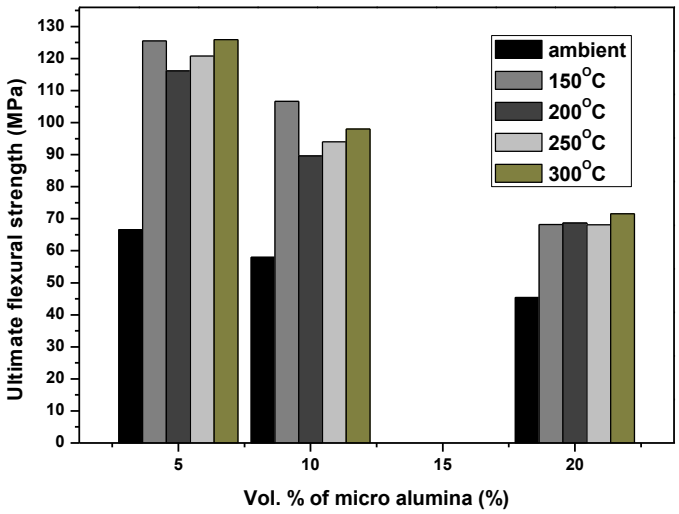

Fig. 4.37 Plot showing the variation of ultimate flexural strength with vol. % of reinforcement for microcomposite after liquid nitrogen quenching

Microcomposites displayed marginally lesser flexural strength than nanocomposites since the brittleness induced in the aluminium matrix due to very high cooling rate permits easy pathway for crack propagation. The plasticity of the matrix surrounding the particle is reduced due to high degree of brittleness. Also, no further enhancement in flexural strength despite very high cooling rate when compared to brine and oil quenching may be due to high dislocation annihilation tendency.

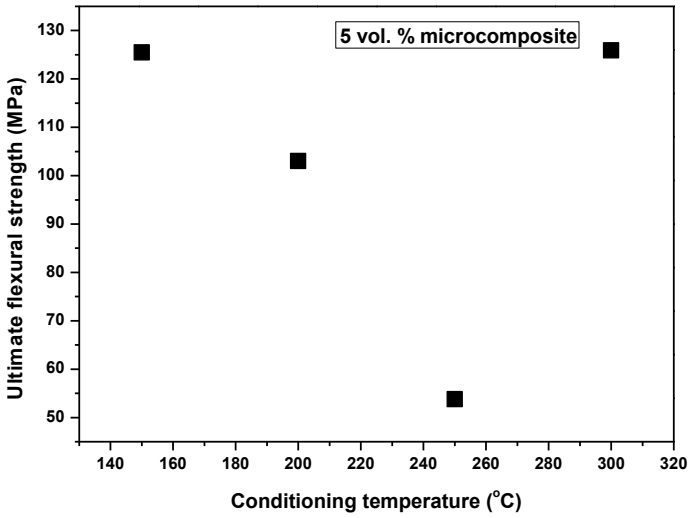

Fig. 4.38 Plot showing the variation of flexural strength with conditioning temperature for 5 vol. % microcomposite after liquid nitrogen quenching

As shown in fig. 4.38, ultimate flexural strength decreased with increasing quenching temperature upto 250°C and thereafter starts increasing. The increase in flexural strength at higher temperature may be due to large number of vacancies generated at high temperature. After quenching these vacancies will be retained in the matrix and can increase the yield strength of the composite.

4.3.2.5 Polymer (PEG-5 vol. %) quenching

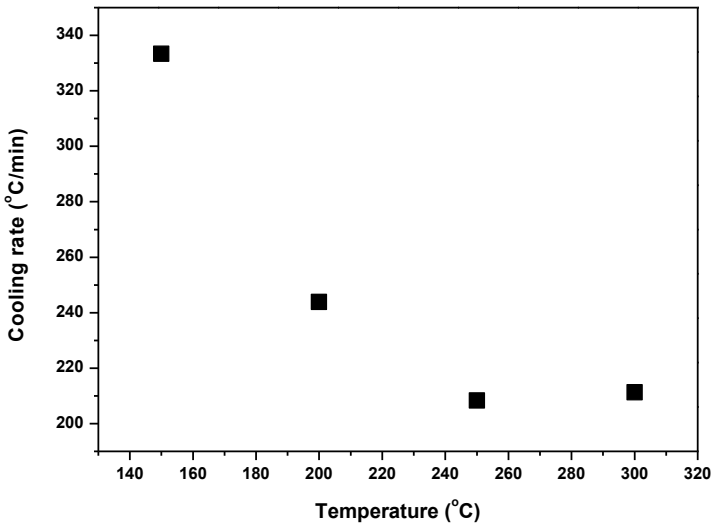

Fig. 4.39 Plot showing the variation of cooling rate with conditioning temperature for polymer quenched specimens

The cooling rate during polymer quenching decreased with increase in quenching temperature. The dissolving of thin film of glycol formed around the specimen will be faster (leading to higher cooling rate) if the temperature of the specimen is more. But, the decrease of cooling rate with temperature displayed here might be due other factors such as, reduced heat transfer coefficient of the polymer, high concentration and non-uniform distribution of the polymer etc.

4.3.2.5.1 Nanocomposite

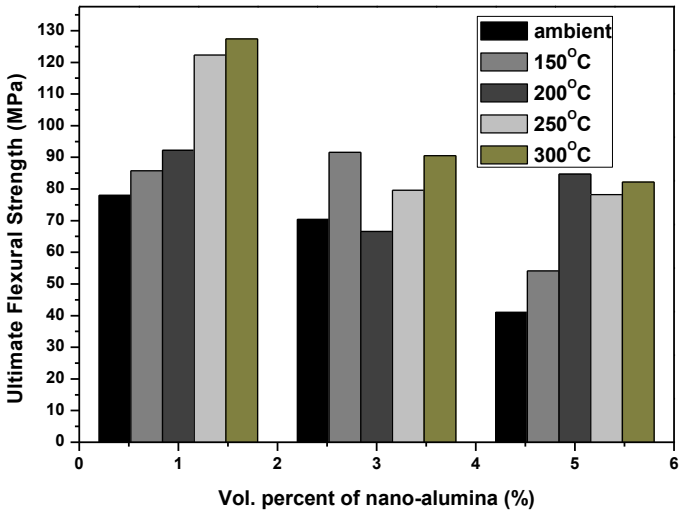

Fig. 4.40 Plot showing the variation of ultimate flexural strength with vol. % of reinforcement for nanocomposite after polymer quenching

Polymer quenching resulted in appreciable enhancement in flexural strength values than ambient values. But the increment in strength was not upto the mark even with high cooling rates of polymer quenching. This may be attributed to the increased dislocation annihilation taking place when dislocation forming tendencies are more. Also, the concentration of the polymer also plays a crucial role. Higher concentration of the polymer can result in lesser strengthening effects due to quenching. The duration of vapour blanket stage would be high if concentration of the polymer is greater. The strength enhancement of nanocomposites occurs due to orowan bowing mechanism, grain refinement and high work hardening rate.

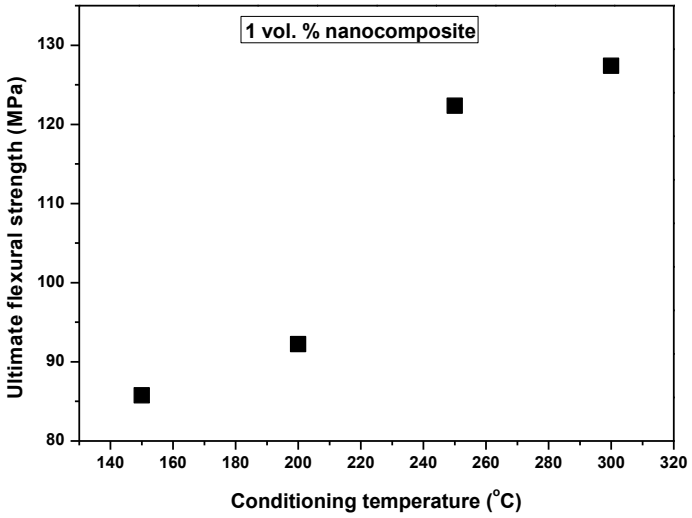

Fig. 4.41 Plot showing the variation of flexural strength with conditioning temperature for 1 vol. % nanocomposite after polymer quenching

The flexural strength of 1 vol. % nanocomposite increased with increasing conditioning temperature. As the heat treatment temperature is more, the thin film of glycol formed around the sample can dissolve at a faster rate increasing the cooling rate. This inturn results in higher dislocation density formation leading to more nanoparticle dislocation interactions. So, the flexural strength of 1 vol. % nanocomposite increases with conditioning temperature during polymer quenching. The FESEM fractography images of PEG quenched nanocomposite in the fig. 4.42 clearly shows the crack propagation path.

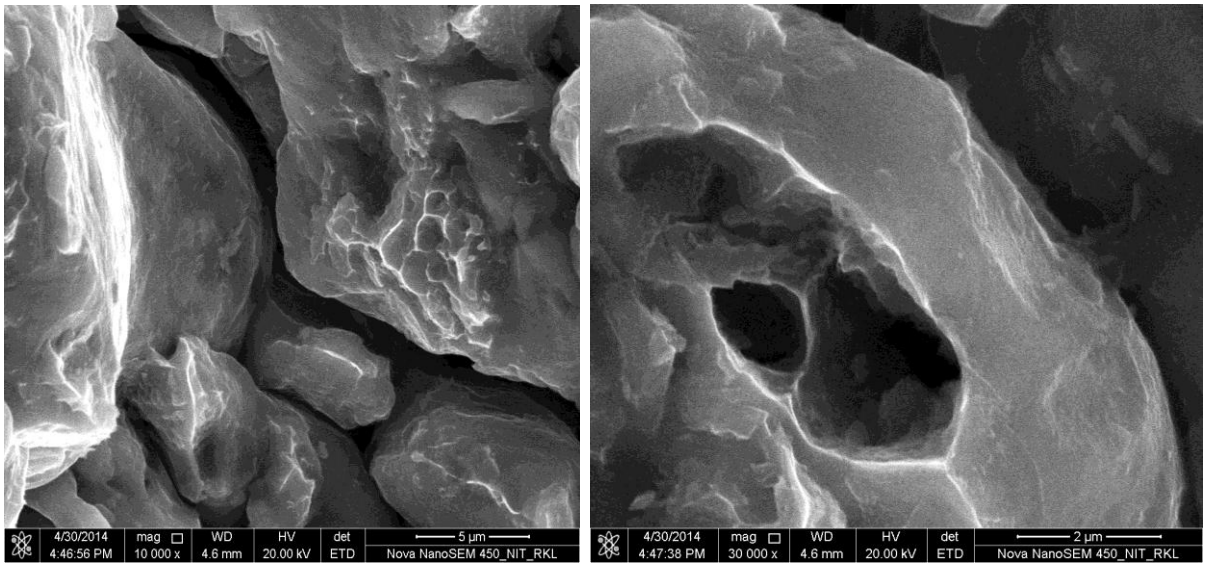

(a) (b)

Fig. 4.42 Fractography of 3-point bend test sample of 5 vol. % nanocomposite quenched in polymer solution from temperature of 300°C shown at (a) 10,000X and (b) 30,000X magnifications.

4.3.2.5.2 Microcomposite

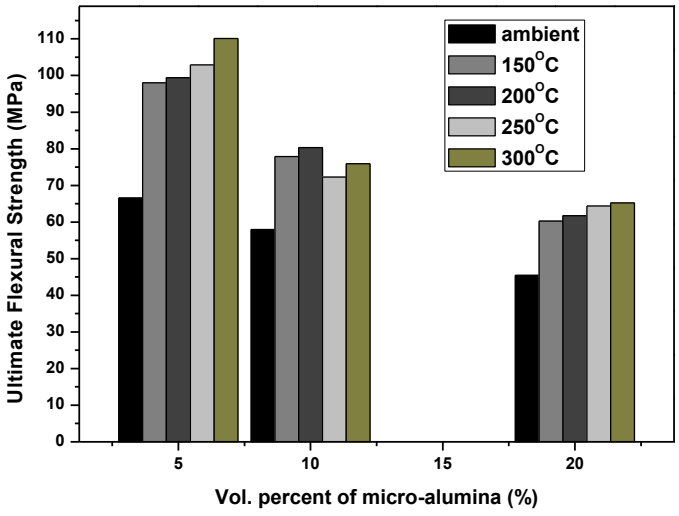

Fig. 4.43 Plot showing the variation of ultimate flexural strength with vol. % of reinforcement for microcomposite after polymer quenching

Eventhough microcomposites quenched in polymer solution displayed higher strength than ambient, their values were lesser than that for air cooling. Generally, polymer quenching produces strength and hardness values intermediate to that of water and oil quenching. Here the decrement of strength may be due to increasing tendency for particle fracture and poor interfacial bonding. The brittleness induced in the matrix due to high cooling rate reduces the plasticity around the regions of stress concentrations near the particles. So crack propagation will be easier through the particles, since the toughening mechanisms such as crack blunting are less operational. With increasing volume fraction of particles, the flexural strength of the microcomposite got reduced due to increase in number of damage accumulation points.

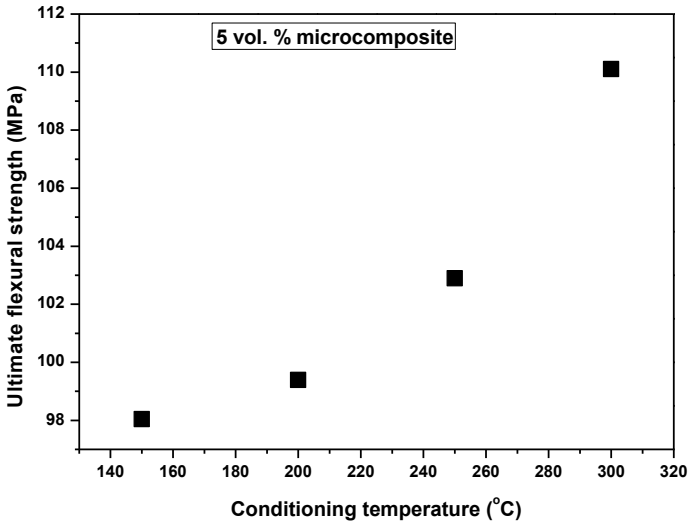

Fig. 4.44 Plot showing the variation of flexural strength with conditioning temperature for 5 vol. % microcomposite after polymer quenching

The flexural strength of 5 vol. % microcomposite increased with increase in conditioning temperature. This trend was similar to the nanocomposites. The decrement in the duration of vapour blanket stage at higher specimen temperatures can be used to explain this behaviour. The cooling power will get enhanced leading to high dislocation density generation due to CTE misfit.

Chapter 5

Conclusions

The effects of quenching media on the mechanical properties of powder metallurgy fabricated Al-Al_2O_3 nano- and microcomposites were studied and the following conclusions were made:-

- Quenching heat treatment has significantly enhanced the hardness and flexural strength of both Al-Al_2O_3 nano- and micocomposites. This improvement can be attributed mainly to two strengthening mechanisms:- (i) large dislocation density developed due to the CTE mismatch between the constituent phases and (ii) back stress developed due to particles blocking the movement of dislocations.
- For all the quenching media used, increase in hardness of composite was observed with increasing volume fraction of reinforcement whereas, decrease in flexural strength was observed with increasing content of reinforcement.
- Air cooling does not result in appreciable increase in strength and hardness of composites due to its low cooling rate.
- Brine quenching showed higher hardness and strength at all conditioning temperatures compared to all other quenchants.
- Maximum cooling rates were observed in liquid nitrogen quenching which induces brittleness in the quenched samples leading to high strength and hardness. But the flexural strength was lower compared to brine water quenching inspite of having higher cooling rate which can be due to increased tendency of dislocation annihilation.
- Oil quenching results in intermediate strength and hardness values due to its lower cooling rates. Increasing the conditioning temperature appreciably increased the flexural strength of composites since the viscosity of oil gets reduced at higher temperatures which facilitates higher cooling rate.
- Polymer quenching unexpectedly resulted in lower hardness and flexural strength values which can be attributed to the increased concentration of the polymer. Increasing polymer concentration can result in lower cooling rates due to the enhanced duration of the vapour blanket stage.

References

[1] T. S. Srivatsan, T. S. Sudarshan, and E. J. Lavernia. "Processing of discontinuously-reinforced metal matrix composites by rapid solidification."*Progress in Materials Science* 39, no. 4 (1995): 317-409.

[2] K. Dash, B. C. Ray, and D. Chaira. "Synthesis and characterization of copper–alumina metal matrix composite by conventional and spark plasma sintering." *Journal of Alloys and Compounds* 516 (2012): 78-84.

[3] M. Gupta, S. Qin, and L. W. Chin. "Effect of particulate type on the microstructure and heat-treatment response of Al-Cu based MMCs", *Journal of material processing and technology*, 65 (1997): 245-251.

[4] M. E. Smagorinski, P. G. Tsantrizos, S. Grenier, A. Cavasin, T. Brzezinski, and G. Kim. "The properties and microstructure of Al-based composites reinforced with ceramic particles." *Materials Science and Engineering: A* 244, no. 1 (1998): 86-90.

[5] Comprehensive of composite materials, volume 6, chapter 6.05 –"Metal matrix composites".

[6] J. S. Shelley, R. LeClaire, and J. Nichols. "Metal-matrix composites for liquid rocket engines." *Journal of Metals* 53, no. 4 (2001): 18-21.

[7] M. M. Sharma, M. F. Amateau, and T. J. Eden. "Aging response of Al–Zn–Mg–Cu spray formed alloys and their metal matrix composites." *Materials Science and Engineering: A* 424, no. 1 (2006): 87-96.

[8] M. K. Surappa, "Aluminium matrix composites: Challenges and opportunities."*Sadhana* 28, no. 1-2 (2003): 319-334.

[9] S. Naher, D. Brabazon, and L. Looney. "Development and assessment of a new quick quench stir caster design for the production of metal matrix composites." *Journal of Materials Processing Technology* 166, no. 3 (2005): 430-439.

[10] O. K. Abubakre, U. P. Mamaki, and R. A. Muriana. "Investigation of the quenching properties of selected media on 6061 aluminum alloy." *Journal of Minerals and Materials Characterization and Engineering* 8 (2009): 303.

[11] A. J. Carver, B. Thomas and A. T. Langton, United States Patent, 1966.

[12] N. R. Prabhuswamy, C. S. Ramesh, and T. Chandrashekar. "Effect of heat treatment on strength and abrasive wear behaviour of Al6061-SiCp composites."*Bulletin of Materials Science* 33, no. 1 (2010): 49-54.

[13] J. Mackerle. "Finite element analysis and simulation of quenching and other heat treatment processes: A bibliography (1976–2001)." *Computational materials science* 27, no. 3 (2003): 313-332.

[14] J. Peng, D. H. W. Li, J. D. Y. Xie, and G. Liu. "Study on the yield behaviour of Al_2O_3-SiO_2 (sf)/Al–Si metal matrix composites." *Materials Science and Engineering: A* 486, no. 1 (2008): 427-432.

[15] R. L. S. Otero, C. F. C. Lauralice, and G. E. Totten. "Use of Vegetable Oils and Animal Oils as Steel Quenchants: A Historical Review-1850- 2010." *Journal of ASTM International* 9, no. 1 (2011): 42-67.

[16] T. V. Rajan, C. P. Sharma, A. Sharma. "Heat treatment principles and techniques", sixth edition, Prentice-Hall of India private limited, New Delhi, 1996.

[17] M. Eshraghi-Kakhki, M. A. Golozar, and A. Kermanpur. "Application of polymeric quenchant in heat treatment of crack-sensitive steel mechanical parts: modeling and experiments." *Materials & Design* 32, no. 5 (2011): 2870-2877.

[18] A. Sharma and S. Das. "Study of age hardening behaviour of Al–4.5 wt% Cu/zircon sand composite in different quenching media–A comparative study." *Materials & Design* 30, no. 9 (2009): 3900-3903.

[19] A. N. Abdel-Azim, Y. Shash, S. F. Mostafa, and A. Younan. "Ageing behaviour of 2024-Al alloy reinforced with Al_2O_3 particles."*Journal of materials processing technology* 55, no. 3 (1995): 140-145.

[20] A. J. Knowles, X. Jiang, M. Galano, and F. Audebert. "Microstructure and mechanical properties of 6061 Al alloy based composites with SiC nanoparticles." *Journal of Alloys and Compounds* (2014): *http://dx.doi.org/10.1016/j.jallcom.2014.01.134.*

[21] J. Eliasson and R. Sandstroem. "Analysis of the coherence of published data on aluminum matrix composites." *Journal of testing and evaluation* 23, no. 4 (1995): 288-294.

[22] K. Dash, S. Panda and B. C. Ray. "Effects of Thermal and Cryogenic Conditionings on Flexural Behavior of Thermally Shocked Cu-Al2O3 Micro and NanoComposites." *Metallurgical and Materials Transactions A* 45, no. 3 (2014): 1567-1578.

[23] R. Kapoor and S. K. Vecchio. "Deformation behaviour and failure mechanisms in particulate reinforced 6061 Al metal-matrix composites."*Materials Science and Engineering: A* 202, no. 1 (1995): 63-75.

[24] M. Gupta, M. O. Lai, M. S. Boon, and N. S. Herng. "Regarding the SiC Particulates Size Associated Microstructural Characteristics on the Aging Behaviour of Al–4.5 Cu Metallic Matrix." *Materials research bulletin* 33, no. 2 (1998): 199-209.

[25] D. Hull and T. W. Clyne. "*An introduction to composite materials."* Cambridge university press, 1996.

[26] T. Christman and S. Suresh. "Microstructural development in aluminium alloy-SiC whisker composite." *Acta metallurgica* 36, no. 7 (1988): 1691-1704.

[27] I. Dutta and D. L. Bourell. "A theoretical and experimental study of aluminium alloy 6061-SiC metal matrix composite to identify the operative mechanism for accelerated aging." *Materials Science and Engineering: A* 112 (1989): 67-77.

[28] R. W. Hertzberg. "*Deformation and fracture mechanics of engineering materials*." Vol. 89. New York: Wiley, 1996.

[29] M. E. Fitzpatrick, M. T. Hutchings, and P. J. Withers. "Separation of macroscopic, elastic mismatch and thermal expansion misfit stresses in metal matrix composite quenched plates from neutron diffraction measurements."*Acta materialia* 45, no. 12 (1997): 4867-4876.

[30] M. Taya, K. E. Lulay, and D. J. Lloyd. "Strengthening of a particulate metal matrix composite by quenching." *Acta metallurgica et materialia* 39, no. 1 (1991): 73-87.

[31] P. Mummery and B. Derby. "The influence of microstructure on the fracture behaviour of particulate metal matrix composites." *Materials Science and Engineering: A* 135 (1991): 221-224.

[32] R. Ikkene, Z. Koudil and M. Mouzali. "Measurement of the Cooling Power of Polyethylene Glycol Aqueous Solutions Used as Quenching Media", *Journal of ASTM International* 7, *No. 2*, (2010): 1–10.

[33] A. J. Fletcher and R. F. Price. "Generation of thermal stress and strain during quenching of low-alloy steel plates." *Metals Technology* 8, no. 1 (1981): 427-446.

[34] T. Croucher. "Minimizing Machining Distortion in Aluminium alloys through Successful Application of Uphill Quenching--A Process Overview." *Journal of ASTM International(JAI)* 1523 (2010): 332-351.

[35] F. S. Allen, A. J. Fletcher, and S. King. "On the quenching characteristics of polyalkylene glycol solutions in water." *Materials science and engineering* 95 (1987): 247-257.

[36] T. E. Hamill, “Aqueous solutions of ethylene glycol, glycerine and sodium silicate as quenching media for steels” *Bureau of journal of research* 7 (1931): 554-560.

[37] T. C. Hua and J. J. Xu. "Quenching boiling in subcooled liquid nitrogen for solidification of aqueous materials." *Materials Science and Engineering: A* 292, no. 2 (2000): 169-172.

[38] Z. Xu and Z. Youxue. "Quench rates in air, water, and liquid nitrogen, and inference of temperature in volcanic eruption columns." *Earth and Planetary Science Letters* 200, no. 3 (2002): 315-330.

[39] K. Prabhu and P. Fernades. "Nanoquenchants for industrial heat treatment." *Journal of Materials Engineering and Performance* 17, no. 1 (2008): 101-103.

[40] K. N. Prabhu and P. Fernandes. "Heat Transfer During Quenching and Assessment of Quench Severity--A Review." *Journal of ASTM International (JAI)* 1523 (2010): 40-62.

[41] X. Luo and G. E. Totten. "Analysis and prevention of quenching failures and proper selection of quenching media: an overview." *Journal of ASTM International* 8, (2011): 4.

[42] F. Ravnik, J. Grum. “Heat transfer stages recognition by boiling acoustic during quenching”, *8*, no. 1 (2014): 1–13.

[43] C. Panseri, F. Gatto, T. Federighi. “The quenching of vacancies in aluminium.” *Acta metallurgica 5*, (1957): 50-52.

[44] F. Bonollo, R. Guerriero, E. Sentimenti, I. Tangerini, and W. L. Yang. "The effect of quenching on the mechanical properties of powder metallurgically produced Al-SiC (particles) metal matrix composites." *Materials Science and Engineering: A* 144, no. 1 (1991): 303-309.

[45] P. Cui, X. S. Guan, and G. Tingsui. "Effect of quenching on grain boundary relaxation in aluminium." *Scripta metallurgica et materialia* 25, no. 12 (1991): 2821-2826.

[46] P. Cui, X. S. Guan, T. S. Kê, and Tingsui Ge. "High-temperature internal friction peak in high-purity aluminium associated with quenching from high temperatures." *Scripta metallurgica et materialia* 25, no. 12 (1991): 2827-2832.

[47] W. DeSorbo, H. N. Treaftis, and D. Turnbull. "Rate of clustering in Al-Cu alloys at low temperatures." *Acta metallurgica* 6, no. 6 (1958): 401-413.

[48] W. DeSorbo and D. Turnbull. "Quenching of imperfections in aluminum." *Acta metallurgica* 7, no. 2 (1959): 83-85.

[49] D. H. Shin and S. W. Nam. "The effect of quenching on static and cyclic creep behavior of pure aluminum and copper." *Scripta Metallurgica* 16, no. 3 (1982): 313-315.

[50] P. Appendino, C. Badini, F. Marino, and A. Tomasi. "6061 aluminium alloy-SiC particulate composite: a comparison between aging behavior in T4 and T6 treatments." *Materials Science and Engineering: A* 135 (1991): 275-279.

[51] P. Fernandes and K. N. Prabhu. "Comparative study of heat transfer and wetting behaviour of conventional and bioquenchants for industrial heat treatment." *International Journal of Heat and Mass Transfer* 51, no. 3 (2008): 526-538.

[52] O. K. Abubakre, U. P. Mamaki, and R. A. Muriana. "Investigation of the quenching properties of selected media on 6061 aluminum alloy." *Journal of Minerals and Materials Characterization and Engineering* 8 (2009): 303.

[53] J. Peng, D. H. W. Li, J. D. Y. Xie, and G. Liu. "Study on the yield behaviour of Al_2O_3-SiO_2 (sf)/Al–Si metal matrix composites." *Materials Science and Engineering: A* 486, no. 1 (2008): 427-432.

[54] S. Pal, R. Mitra, and V. V. Bhanuprasad. "Aging behaviour of Al–Cu–Mg alloy–SiC composites." *Materials Science and Engineering: A* 480, no. 1 (2008): 496-505.

[55] W. Cheng, Y. Lin, C. Liu. The fracture behaviours in a Fe-Mn-Al alloy during quenching processes, *Materials Science and Engineering A343 (2003) 28-35.*

[56] V. V. Prasad, B. V. R. Bhat, Y. R. Mahajan, and P. Ramakrishnan. "Structure–property correlation in discontinuously reinforced aluminium matrix composites as a function of relative particle size ratio." *Materials Science and Engineering: A* 337, no. 1 (2002): 179-186.

[57] N. E. Bekheet, R. M. Gadelrab, M. F. Salah, and A. N. Abd El-Azim. "The effects of aging on the hardness and fatigue behavior of 2024 Al alloy/SiC composites." *Materials & design* 23, no. 2 (2002): 153-159.

[58] L. Pedersen and L. Arnberg. "The effect of solution heat treatment and quenching rates on mechanical properties and microstructures in AlSiMg foundry alloys." *Metallurgical and Materials Transactions A* 32, no. 3 (2001): 525-532.

[59] V. K. Varma, Y. R. Mahajan, and V. V. Kutumbarao. "Ageing behaviour of Al-Cu-Mg alloy matrix composites with SiC particle of varying sizes."*Scripta materialia* 37, no. 4 (1997): 485-489.

[60] M. P. Thomas and J. E. King. "Quench sensitivity of 2124 Al alloy and Al/SiCp metal matrix composite." *Scripta metallurgica et materialia* 31, no. 2 (1994): 209-214.

[61] S. I. Hong, G. T. Gray, and K. S. Vecchio. "Quenching and thermal cycling effects in a 1060-Al matrix-10vol. % Al_2O_3 particulate reinforced metal matrix composite." *Materials Science and Engineering: A* 171, no. 1 (1993): 181-189.

[62] P. Cui, X. S. Guan, and G. Tingsui. "Effect of quenching on grain boundary relaxation in aluminium." *Scripta metallurgica et materialia* 25, no. 12 (1991): 2821-2826.